California State University, Monterey Bay
Digital Commons @ CSUMB

Capstone Projects and Master's Theses

2007

A 300-year geochronological assessment of atmospheric mercury depostition in California

Rhea D. Sanders
California State University, Monterey Bay

Recommended Citation

Sanders, Rhea D., "A 300-year geochronological assessment of atmospheric mercury depostition in California" (2007). *Capstone Projects and Master's Theses*. 81.
https://digitalcommons.csumb.edu/caps_thes/81

A 300-YEAR GEOCHRONOLOGICAL ASSESSMENT OF ATMOSPHERIC MERCURY DEPOSITION IN CALIFORNIA

A Thesis

Presented to

The Faculty of Moss Landing Marine Laboratories

California State University Monterey Bay

In Partial Fulfillment

of the Requirements for the Degree

Master of Science

By

Rhea D. Sanders

May 2007

APPROVED FOR MOSS LANDING MARINE LABORATORIES

Kenneth H. Coale

Dr. Kenneth H. Coale, Professor

Dr. Ivano Aiello, Professor

Dr. Michael Graham, Professor

APPROVED FOR THE UNIVERSITY

Dr. Steve Moore, Professor

ABSTRACT

A 300-YEAR GEOCHRONOLOGICAL ASSESSMENT OF ATMOSPHERIC MERCURY DEPOSITION IN CALIFORNIA

by Rhea D. Sanders

Aquatic mercury (Hg) contamination and subsequent bioaccumulation pose a threat to human and ecosystem health. The mitigation of contaminated water bodies requires an understanding of natural baselines of metal concentrations and fluxes. In this study, six age-dated sediment cores were analyzed to assess temporal and spatial variability of atmospheric Hg deposition from remote natural lakes throughout California. Geochemical proxies, including ^{210}Pb, particle size, magnetic susceptibility, organic carbon and organic nitrogen, were measured to apportion Hg concentrations between atmospheric deposition, anthropogenic and watershed processes. Anthropogenic Total Hg (Hg_T) lake sediment concentrations increased by factors of 2 to 10 times that of historic (pre-1850) Hg_T concentrations in all four lakes studied. Results support the hypothesis that atmospheric Hg deposition, and its subsequent flux to lake sediments, was the cause of elevated Hg levels and that regional sources, from both abandoned mine sites and industrial emissions, were a major source of biologically available Hg to aquatic ecosystems in California. Hence, the past biotic exposure, if scaled relative to the measured deposition, would have been 2, 5, and 10 times lower than present day levels for coastal, Central Valley, and Coastal Range aquatic systems, respectively. These values may be useful benchmarks for the development of site-specific mitigation strategies for contaminated watersheds.

ACKNOWLEDGEMENTS

I would like to thank Dr. Kenneth Coale for compelling me to conduct this study and for all his mentoring in the field, lab, and shop. Thanks to my other thesis committee members, Dr. Ivano Aiello and Dr. Mike Graham, for all their support and expertise. I would also like to express my gratitude to Dr. Chris Foe who provided initial inspiration to design a historic atmospheric mercury study to support TMDL regulations.

This project could not have been completed without the support of my lab-mates Elizabeth Sassone, Tom Kimball, Allison Myers, and Berkeley Kauffman. I would especially like to express my warmest appreciation to Tam Voss who assisted in mercury analysis and fieldwork on her limited spare time. I owe many thanks to the remaining 'mercury group', Gary Gill, Ron Lehman, Key Young Choe, Wes Heim, Mark Stephenson *et al.*, for all their expertise and atmospheric wet deposition support. Andrew Thurber, Annie Kimball and my sister Shawne Sanders provided additional field support.

Many Moss Landing Marine Lab researchers trained and supported the analytical work for this study. Thanks to Allen Andrews for sharing his radiochemistry resources and expertise and always being so accommodating. Craig Hunter was kind enough to train and assist in particulate organic carbon analysis. And thanks again to Ivano Aiello for offering his lab and equipment to conduct the remaining geologic characterization and his contagious enthusiasm for mud.

I owe a sincere thanks to all of Moss Landing faculty and staff especially Joan Parker and other library staff for always acquiring obscure grey literature when requested, the IT staff, Jeff Arlt, Brandon Rose, and John Witkowski, who kept us all connected. Thank you to all my fellow Moss Landing students and friends.

I would like to thank all those who employed and supported me during my studies including the Moss Landing Marine Pollutions Lab, the Benthic Lab, and most of all John Haskins at the Elkhorn Slough Reserve who demonstrated so much support and flexibility while I was completing my degree.

I would like to offer my appreciation to Diana Humple of PRBO for all her volunteer hours helping with the Atmospheric collector. She is a volunteer coordinator who is not afraid to volunteer.

Finally, I owe my family and friends many thanks for all of their love and support during my studies.

This research was supported by Regional Board contract 01-281-150-2 awarded to the San Jose State University Foundation. Packard Travel Grant, International Mercury Under Represented Group Scholarship, and NSF Research Collaboration Grant provided additional fiscal support.

CONTENTS

CHAPTER 2 – A 300-year geochronological assessment of atmospheric mercury deposition in California

LIST OF TABLES

Table

LIST OF FIGURES

Figure

CHAPTER 1

General Introduction:
Biogeochemical Cycling of Mercury

The bioaccumulation of mercury (Hg) in aquatic systems is controlled by complex biogeochemical reactions that require trace amounts of Hg (e.g. Gill and Bruland, 1990; Fitzgerald *et al.,* 1998). In California, elevated Hg concentrations found in biota downstream from historic gold (Au) and Hg mines are thought to originate from remaining Hg contaminated mine tailings (Alpers *et al.,* 2004). Elevated Hg levels, however, have been identified in water bodies without associated mine site runoff (point source), indicating a non-point source of Hg to aquatic systems. Elevated atmospheric Hg deposition is suspected to be partially responsible for elevated Hg concentrations found throughout California aquatic biota. Atmospheric Hg deposition supplies the most readily available form of Hg, Hg (II), for methylation and subsequent bioaccumulation in aquatic systems. An understanding of Hg sources, sinks and pathways is needed to understand the impacts associated with elevated levels of Hg in the environment.

Relative contributions of anthropogenic and natural mercury emissions to the atmosphere are poorly understood. The major anthropogenic sources of global Hg are coal-fired power plants, industrial boilers, municipal waste combustors, medical waste incinerators, and other sources (USEPA, 1997). Estimates of anthropogenic Hg emissions in North America identify electric utilities, waste incineration, coal burning, mining, chlor-alki facilities, automobiles, and other sources as the primary origins (Mason *et al.*, 1994).

Global natural Hg emissions consist of mercury-enriched geologic sources, volcanic emissions, oceans, and vegetation fires (USEPA, 1997). Ocean ridges and oceanic crust are possible natural geologic sources of Hg, however, full depth seawater profiles for mercury do not show significant increases in deep water, indicating that these regions contribute relatively small amounts to the global budget (Fitzgerald *et al.,* 1998). Hg released from ocean tectonic areas appear to be scavenged by precipitating iron (Fe) and Manganese (Mn) near vents (Fitzgerald *et al.,* 1998). Plate tectonic activity and subsequent geologic Hg releases have been relatively stable over the short geologic time scale of the industrial revolution (Fitzgerald *et al.,* 1998). The evasion of Hg (elemental) from the oceans is balanced by total oceanic atmospheric Hg (II) deposition (Mason *et al.*, 1994). Finally, terrestrial vegetation takes up Hg from the atmosphere that is subsequently released back to the atmosphere during forest fires (Lindberg and Turner, 1988). Estimates of the global Hg budget is continually being adjusted as researchers attempt to quantify Hg emissions applying new technology and discovering new sources. The estimates of the relative contribution of anthropogenic and natural inputs to the global Hg budget are particularly variable (Seigneur *et al.,* 2004).

The primary mechanism for global Hg transport is atmospheric mobilization and deposition (Lindberg and Turner, 1988; Bloom and Watras, 1989; Fitzgerald *et al.*, 1998). Hg resides at varying levels in the atmosphere depending on its form (Lindberg and Turner, 1988). The majority of atmospheric Hg resides in the upper troposphere as elemental Hg (Hg^0) for approximately 1.3 years and is distributed globally; Hg sulfide, chloride, and oxides, or inorganic Hg (II), reside in the lower troposphere for days and are deposited regionally within 100-1000 km of the source. Particulate bound Hg is deposited locally, less than 100 km, within hours (Andreae *et al.*, 1984; Lindberg and Turner, 1988). The long residence time in the troposphere allows elemental Hg to be widely dispersed across the earth's surface including remote regions (Fitzgerald *et al.,* 2005). Clouds and scavenging aerosols ultimately oxidize Hg^0 and convert to reactive Hg forms (e.g. Hg (II), $HgCl_2$, $Hg(OH)_2$), that are subsequently deposited (Mason *et al.,* 1994). The dominant sink for atmospheric Hg appears to be on land rather than over the ocean (Mason *et al.,* 1994). Global-scale processes dominate atmospheric Hg deposition concentrations, however, significant regional sources can cause increases over the global background rates (Nater and Grigal, 1992).

Major regional reservoirs of Hg in California exist as naturally occurring cinnabar (HgS) deposits. The northern California coast range is one of three geologic Hg belts in the world and is a major source of regional atmospheric Hg in California (Gustin, 2003). The Hg belts are located along plate boundaries associated with volcanic and geothermal activity that release Hg to the atmosphere. Coast range cinnabar was heavily mined, beginning around 1850, to support gold mining operations (Heyvaert *et al.,* 2000). Currently, emissions from historic mine sites are suspected to be major contributors of mercury to the atmosphere (Coolbaugh *et al.*, 2002; Gustin, 2003; Nacht *et al.*, 2004).

Bioaccumulation and the associated toxic effects of Hg in aquatic systems represent a potential risk to human health and the environment (e.g. Alpers *et al.*, 2004). Hg toxicity not only affects humans, but leads to reproductive failure among piscivorous species (Uryu *et al.*, 2001). Fish continually accumulate methyl Hg (MeHg) over time because they lack the demethylating mechanism found in many marine mammals, thus resulting in substantial Hg amassing in longer lived and high trophic level species (Trudel and Rasmussen, 2001). MeHg and other organic Hg forms readily bioaccumulate in aquatic systems and impact environmental and public health. MeHg in fishes is currently of particular concern because it represents the most common source of Hg to humans (Trudel and Rasmussen, 2001). In an attempt to protect against Hg poisoning, the EPA has set a suggested maximum dose of 0.1 ppm MeHg per day whereas the National Academy of Sciences suggest a maximum of 0.3 ppm MeHg per day (USEPA, 1997).

As monitoring efforts increase, more lakes and rivers are issued fish advisories (USEPA, 2004). Elevated Hg in game fishes (exceeding 0.5-1.0 ppm wet-wt. muscle) in north-central Wisconsin lakes is thought to originate from atmospheric sources (Rada *et al.*, 1989). Forty percent of sampled fish, walleyes *(Stizostedion vitreum),* were demonstrated to have elevated Total Hg (Hg_T) levels (exceeding 0.5 ppm wet-wt.) despite low mercury concentrations in the water column (Barbiarz and Andren, 1995); Hg_T is a mixture of Hg species including organic and inorganic complexes (Tseng *et al.*, 2004). In addition to other environmental variables, the lack of correlation between fish and water concentrations is likely due to the major form of atmospheric Hg, Hg (II), which is quickly scavenged or evaded from the water column by several processes and is ultimately deposited to sediments. Johnson *et al.* (1987) correlated Hg loading rates using ^{210}Pb dated lake sediment cores with concentrations in several fishes from 14 Ontario Lakes where the main source was determined to be anthropogenic atmospheric Hg deposition. Johnson *et al.* (1987) demonstrated that sediments are a more representative medium to analyze than water when investigating the correlation between atmospheric deposition and biotic exposure.

It is difficult to regulate Hg pollution since atmospheric emissions, from both point and non-point sources, can be distributed globally. An understanding of the historic (pre-industrial) and modern (post-industrial) biogeochemical cycling of Hg are needed to set realistic limits for informed mitigation and resource management. Uncertainties exist in the understanding of natural Hg levels, the geographic origin of elevated Hg (thus obscuring the source responsible for elevated Hg) and location where remediation efforts should be focused. For example, the Environmental Protection Agency (EPA) recently relaxed regulations on U.S. coal burning emissions because of controversy over whether elevated Hg levels in Americans are caused by consumption of local fishes or fishes from overseas (USEPA, 2005). Atmospheric Hg deposition needs to be quantified in order to support resource managers and agencies in identifying sources of pollution and how to regulate emissions. In this study, lake bottom cores from remote regions throughout California, representing distinct biogeochemical/industrial provinces, were collected, sectioned, dated and analyzed to assess historic biotic exposure. The next chapter was formatted after the journal requirements (Applied Geochemistry) to which this study was submitted.

References

Alpers, C. N., Hunerlach, M. P., May, J. T., Hothem, R. L., Taylor, H. E., Antweiler, R. C., De Wild, J. F., Lawler, D. A, 2004. Geochemical characterization of water, sediment, and biota affected by mercury contamination and acidic drainage from historical gold mining, Greenhorn Creek, Nevada County, California, 1999-2001. US Geol. Surv. Open-File Report, 2004-5251, 278.

Andreae, M. O., Asami, T., Bertine, K. K., Buat-Ménard P. E., Duce, R. A., Filip, Z., Förstner, U., Goldberg, E. D., Heinrichs, H., Jernelöv, A. B., Pacyna, J. M., Thornton, I., Tobschall, H. J., Zoller, W. H., 1984. Changing biogeochemical cycles (group report). In: J. O. Nriagu (Ed.), Changing metal cycles and human health. Dahlem Konferenzen. Berlin, Heidelberg, New York, Tokyo: Springer-Verlag, pp. 359-373.

Babiarz, C. L., Andren, A. W., 1995. Total concentrations of mercury in Wisconsin (USA) lakes and rivers. Water Air Soil Pollut., 83, 173-183.

Bloom, N. S., Watras, C. J., 1989. Observations of methylmercury in precipitation. Sci. Total Environ., 87/88, 199-207.

Coolbaugh, M. F., Gustin, M. S., Rytuba, J. J., 2002. Annual emissions of mercury to the atmosphere from natural sources in Nevada and California. Environ. Geol., 42, 338-349.

Fitzgerald, W. F., Engstrom, D. R., Mason, R. P., Nater, E. D., 1998. Critical Review: The Case for Atmospheric Mercury Contamination in Remote Areas. Environ. Sci. Technol. 32(1), 1-7.

Fitzgerald, W. G., Engstrom, D. R., Lamborg, C. H., Tseng, C., Balcom, P. H., Hammershmidt, C. R., 2005. Modern and historic atmospheric mercury fluxes in Northern Alaska: Global sources and arctic depletion. Environ. Sci. Technol., 39, 557-568.

Gill, G. A., Bruland K. W., 1990. Mercury speciation in surface freshwater systems in California and other areas. Environ. Sci. Technol., 24(9), 1392-1400.

Gustin, M.S., 2003. Are mercury emissions from geologic sources significant? A status report. Sci. Total Environ., 304, 153-167.

Heyvaert, A. C., Reuter, J. E., Slotton, D. G., Goldman, C. R., 2000. Paleolimnological reconstruction of historical atmospheric lead and mercury deposition at Lake Tahoe, California-Nevada. Environ. Sci. Technol., 34, 3588-3597.

Johnson, M. G., 1987. Trace element loadings to sediments of fourteen Ontario lakes and correlations with concentration in fish. Can. J. Fish. Aquat. Sci., 44, 3-13.

Lindberg, S. E., Turner, R. R., 1988. Factors influencing atmospheric deposition, stream export, and landscape accumulation of trace metals in forested watershed. Water Air Soil Pollut., 39 (1-2), 123-156.

Mason, R. P., Fitzgerald, W. F., Morel, F. M. M., 1994. The biogeochemical cycling of elemental mercury: Anthropogenic influences, Geochim. Cosmochim. Acta, 58(15), 3191-3198.

Nacht, D. M., Gustin, M. S., Engle, M. A., Zehner, R. E., Giglini, A. D., 2004. Atmospheric mercury emissions and speciation at the Sulphur Bank mercury mine superfund site, Northern California. Environ. Sci. Technol., 38, 1977-1983.

Nater, E. A., Grigal, D. F., 1992. Regional trends in mercury distribution across the Great Lakes states, north central USA. Nature, 358, 139-141.

Rada, R. G., Wiener, J. G., Winfrey, M. R., Powell, D. E., 1989. Recent increases in atmospheric deposition of mercury to North-Central Wisconsin lakes inferred from sediment analyses. Arch. Environ. Contam. Toxicol., 18, 175-181.

Seigneur, C., Vijayaraghavan, K., Lohman, K., Karamchandani, P., Scott, C., 2004. Global source attribution for mercury deposition in the United States. Environ. Sci. Technol., 38, 555-569.

Trudel, M., Rasmussen, J. B., 2001. Predicting mercury concentration in fish using mass balance models. Ecolog. App., 517-529.

Tseng, C. M., Lamborg, C., Fitzgerald, W. F., Engstrom, D. R., 2004. Cycling of dissolved elemental mercury in Arctic Alaskan lakes. Geochim. Cosmochim. Acta, 68(6), 1173-1184.

Uryu, Y., Malm, O., Thornton, I., Payne, I., Cleary, D., 2001. Mercury contamination of fish and its implications for other wildlife of the Tapajós Basin, Brazilian Amazon. Cons. Biol., 15, 438-446.

U. S. Environmental Protection Agency (USEPA), 1997. Mercury study: Report to Congress. Office of Air Quality Planning and Standards. Office of Research and Development. Washington, D.C., EPA-452/R-97-003.

U. S. Environmental Protection Agency (USEPA), 2004. The national listing of fish advisories. http://www.epa.gov/waterscience/fish/advisories, 134.67.99.49.

U. S. Environmental Protection Agency (USEPA), 2005. Proceedings and summary report: Workshop on the fate, transport, and transformation of mercury in aquatic and terrestrial systems. CLARIT Web Print, 625R02005.

CHAPTER 2

A 300-year geochronological assessment of atmospheric mercury deposition in California

Submitted February 28, 2007

1. Abstract

Aquatic mercury (Hg) contamination and subsequent bioaccumulation pose a threat to human and ecosystem health. The mitigation of contaminated water bodies requires an understanding of natural baselines of metal concentrations and fluxes. In this study, six age-dated sediment cores were analyzed to assess temporal and spatial variability of atmospheric Hg deposition from remote natural lakes throughout California. Geochemical proxies, including ^{210}Pb, particle size, magnetic susceptibility, organic carbon and organic nitrogen, were measured to apportion Hg concentrations between atmospheric deposition, anthropogenic and watershed processes. Anthropogenic Total Hg (Hg_T) lake sediment concentrations increased by factors of 2 to 10 times that of historic (pre-1850) Hg_T concentrations in all four lakes studied. Results support the hypothesis that atmospheric Hg deposition, and its subsequent flux to lake sediments, was the cause of elevated Hg levels and that regional sources, from both abandoned mine sites and industrial emissions, were a major source of biologically available Hg to aquatic ecosystems in California. Hence, the past biotic exposure, if scaled relative to the measured deposition, would have been 2, 5, and 10 times lower than present day levels for coastal, Central Valley, and Coastal Range aquatic systems, respectively. These values may be useful benchmarks for the development of site-specific mitigation strategies for contaminated watersheds.

2. Introduction

As a result of anthropogenic activities, mercury (Hg), a toxic metal, has been released to the atmosphere at an accelerated rate from natural geologic sources worldwide. Much of the elevated total Hg (Hg_T) concentrations in California aquatic environments have been attributed to vast amounts of Hg released during the historic California gold rush (May *et al.*, 2000; Churchill and Clinkenbeard, 2003; Alpers *et al.*, 2004; Slowey *et al.*, 2005). Modern gaseous emissions and particulate suspension from abandoned gold and mercury mine sites and natural geothermal areas across California are now suspected to contribute to elevated regional atmospheric Hg (Coolbaugh *et al.*, 2002; Gustin, 2003; Nacht *et al.*, 2004). In addition, industrial point sources, such as coal combustion, medical incineration, and other municipal waste combustions, have increased global and regional atmospheric Hg concentrations in precipitation (Mason *et al.*, 1994; USEPA, 1997; Fitzgerald *et al.*, 1998; USEPA, 2005).

The well being of Native American tribes and other artisanal fishers are being significantly affected by fish consumption advisories nationwide (Wheatley, 1997). Native American tribes around Clear Lake, CA demonstrated elevated levels of organic Hg in their blood (15.6 μg/L (n=56); Harnly *et al.*, 1997). A large portion of their diet consisted of local fish with Hg levels >1 μg/g (Harnly *et al.*, 1997). Controversy arose from questioning whether the elevated Hg in Clear Lake fish were from surrounding Super Fund mine sites or atmospheric Hg deposition from global sources. Alternatively, because of its geologic and hydrothermal setting, fish in Clear Lake were suspected to have naturally high levels of Hg (Harnly *et al.*, 1997).

Lakes can provide reliable estimates of historic Hg concentrations by preserving the flux of Hg from atmospheric deposition to sediments through time. Several studies have been conducted in various regions around the world in an attempt to quantify the atmospheric deposition of Hg before and after the industrial revolution by utilizing lake basins as atmospheric deposition catchments (Table 1). Most metals, including Copper (Cu), Nickel (Ni), Zinc (Zn), Lead (Pb), Cadmium (Cd), Chromium (Cr), and Hg, do not appear to migrate or redistribute within sediments, or between sediments and the overlying water, once deposited unless sediments are subject to bioturbation (Johnson *et al.*, 1986). Exceptions include Fe and Mn, which migrate upward from reducing to oxidizing sites (Johnson *et al.*, 1986). Atmospheric Hg is mainly deposited as oxidized Hg, Hg (II), which is relatively immobile once deposited to lake sediments because it is strongly bound to organic material (Lucotte *et al.*, 1995). Based on historic information from sediment cores in lakes worldwide, atmospheric deposition of Hg has increased by at least a factor of two relative to natural levels since the industrial revolution (beginning of the 20th century); however, lakes in closer proximity to industrial point sources demonstrated enrichment levels that were greater (Rada *et al.*, 1989; Nater and Grigal, 1992; Mason *et al.*, 1994; Lucotte *et al.*, 1995; Fitzgerald *et al.*, 1998; Fitzgerald *et al.*, 2005). Because of this regional factor, it is critical to conduct regional lake studies to ascertain the spatial and temporal variability in atmospheric Hg deposition.

Sediment studies have been conducted in California to estimate rates of Hg deposition. Heyvaert *et al.* (2000) obtained sediment cores from Lake Tahoe, California and found that Hg_T concentrations in sediments have increased by a factor of 6 since

1850. Suchanek *et al.* (1997) collected sediment cores from Clear Lake, California and found Hg_T concentrations in sediments climbed by a factor of 5 to 10 above natural levels since an approximate date of 1927. Confounding factors in these lakes, however, are suspected to have caused an overestimation of Hg fluxes. Lake Tahoe is a large lake with a high degree of spatial and temporal variability in sediment deposition; logging operations within the watershed may have accelerated nutrient loading (Heyvaert *et al.*, 2000). Similarly, Clear Lake was subjected to direct input of Hg from extensive mine operation tailing deposits (Suchanek *et al.*, 1997). Mercury levels in sediment cores from San Francisco Bay were 20 times greater than baseline levels between 1850 and 1880 and the increase was attributed to the debris from hydraulic gold mining (Hornberger *et al.,* 1999). Although these studies indicated Hg was elevated from natural levels due to mining, the enrichment factors may have been overestimated and the studies did not apportion atmospheric deposition to local or regional sources.

Potential atmospheric Hg inputs to California include global, regional, and local sources. Wang *et al.* (2000) estimated that 2,500 tons of mercury was emitted into the atmosphere during coal combustion processes from 1978 to 1995 in China. A study conducted at the Mt. Bachelor Observatory traced major plumes of Asian industrial emissions containing Hg being deposited on the west coast of North America (Weiss-Penzias *et al.,* 2000). Major regional reservoirs of Hg in California exist as naturally occurring cinnabar (HgS) deposits. The northern California coast range is one of three geologic Hg belts in the world that are suspected to be a major source of regional atmospheric Hg (Gustin, 2003). The Hg belts are located along plate boundaries associated with volcanic and geothermal activity that release Hg to the atmosphere. Coast range cinnabar was heavily mined, beginning around 1850, to support gold mining operations. Twelve million kilograms of Hg was used in gold mining activities during 1860-1900. Approximately 10-30% of the mined Hg was lost to the environment during processing and 60% of the lost Hg was released to the atmosphere (Heyvaert *et al.,* 2000). Emissions from abandoned mine sites are suspected to be significant contributors of mercury to the regional atmosphere (Coolbaugh *et al.*, 2002; Gustin, 2003; Nacht *et al.*, 2004). The relative contributions of global, regional, and local Hg inputs to atmospheric Hg deposition have not been apportioned in California.

Many studies have identified atmospherically derived Hg as the major source of Hg to remote lakes, but have not identified the mechanisms of deposition (Morel *et al.*, 1998; Schwesig *et al.*, 1999; Vaidya *et al.*, 2000). Atmospherically deposited Hg enters water bodies through two main pathways, direct and indirect input. Direct Hg input is atmospheric deposition onto water surfaces while indirect Hg input is Hg deposited on surrounding watersheds that eventually runs off into aquatic systems. The portion of Hg that binds to watershed soils and vegetation versus that portion that runs off into aquatic systems are poorly apportioned (Hintelmann *et al.*, 2002).

Several watershed components and/or proxies were analyzed in this study in order to estimate watershed and atmospherically derived Hg to lake sediments including magnetic susceptibility, particle size, and organic carbon and nitrogen. Characterization of sediment composition provides indications of past conditions that may influence Hg_T concentration in lake sediments (Best *et al.,* 1996; Bilali *et al.,* 2002; Stevenson *et al.,* 2001; Scholz *et al.,* 2003; Marchetto *et al.,* 2004). The relative apportioning of direct and indirect atmospheric deposition can be ascertained by determining the correlation between watershed and atmospheric components.

Currently, the relative contribution of global, regional, and local non-point and point atmospheric sources to aquatic systems of California remain unknown thus hindering a cost-benefit analysis of management measures that would have the greatest impact on decreasing Hg inputs to California water bodies. The objectives of this study were to begin to address these discrepancies in the state of California by: 1) quantifying Hg enrichment factors from historic, pre-industrial (prior to 1850) to modern, post-industrial atmospheric Hg deposition using lake sediment cores (temporal variability), 2) comparing modern Hg enrichment factors among lakes to determine if regional atmospheric Hg enrichment is greater than the estimated global enrichment (spatial variability), 3) determining the relative contributions of watershed and lake processes to lake sediment Hg concentrations, and 4) estimating mass Hg loadings for each lake system.

3. Experimental Methods

3.1. Study Area

Lakes selected for this study met strict criteria to accurately represent atmospheric Hg deposition trends and to avoid confounding factors that include drainage basin characteristics and proximity to Hg sources. Lakes with relatively small drainage basin to lake surface area and low topographic relief were ideal candidates for this study because of the lower runoff input; hence, most of the Hg deposition could be attributed to atmospheric sources. Lakes with most of these characteristics were identified using USGS topographical maps of California. Small, natural, catchments with SCUBA diving depths (<10 m) and gently sloped bottom bathymetry were chosen. Level and uniform bathymetry decreases focusing factors and results in more evenly dispersed sediments over the lake bottom (Fitzgerald *et al.*, 2005). Lakes were also selected at or near headwaters of watersheds to avoid anthropogenic point sources. The drainage basins were selected to be absent of known point source Hg contamination, such as residential or industrial practices that include Hg and gold mines. Deforestation or livestock grazing can accelerate lake sedimentation rates; resulting in dilution of the anthropogenic signal or concentration of organic bound Hg (Fitzgerald *et al.*, 2005); therefore, lake sites were chosen where watersheds were relatively undisturbed by land use practices for the last two hundred years to support the assumption that the sedimentation rate was constant. The geologic composition and activity for each lake was considered because the existence of naturally occurring Hg introduced through hydrothermal activity or cinnabar (HgS) deposits within a watershed could elevate Hg in the lake sediments.

Westerly prevailing wind trajectories in Central California were utilized to identify four lakes, with the previously defined characteristics, downwind of: 1) global sources (Central Coast California; Wildcat Lake), 2) local Hg mine and naturally occurring Hg deposit sources (Northern California Coast Range; Castle Lake), 3) local gold mine sources (Northern Sierra-Nevadas; Island Lake), and 4) regional sources (Southern Sierra-Nevadas; Emerald Lake; Figure 1; Hayes *et al.,* 1984; WRCC, 2001).

Wildcat Lake is located along the coast of California in Point Reyes National Seashore and was chosen to represent the global atmospheric Hg signal from across the Pacific Ocean (Table 2; Figure 2). The lake is perched on the edge of the California coastline and is influenced primarily by onshore winds. The Wildcat Lake drainage basin has low topographic relief with shrubby vegetation to the waters edge. The surrounding geology is composed of granites and shales. Bathymetry is characterized by gradually sloping sides to a relatively shallow center (10 m). Below the epilimnon, Wildcat Lake is depleted in oxygen and concomitantly enriched in sulfides.

Castle Lake is located near Hg and gold mines in the Klamath-Trinity Mountain Coast range, but no mines exist in the watershed. Castle Lake was chosen to characterize an atmospheric Hg baseline amidst the naturally occurring cinnabar deposits. It is surrounded by steep granitic outcrops on the southern end and gradual vegetated slopes on the northern end (Table 2; Figure 3). The southern end of the lake bathymetry drops off abruptly and the Northern end slopes gradually and contains a series of flat shelf areas.

Island Lake is located downwind of the most heavily gold mined area in California, on the Grouse Ridge of the Sierra-Nevadas, but no mines exist in the watershed (Table 2; Figure 4). Island Lake was selected to quantify local atmospheric inputs of abandoned hydraulic gold mines. It has a high lake to basin area ratio, which decreases the runoff potential from the surrounding watershed and supports atmospheric deposition as the main source of Hg to lake sediments. The lake is located in a shallow granitic basin that is sparsely vegetated with high alpine shrubs and pine trees. No bathymetry records existed for this lake; therefore, the coring sight was chosen by exploration until a shallow shelf area was found.

Emerald Lake is located in the Sequoia National Park and was selected to represent regional background atmospheric input because there is a lack of local mining activity. The lake has high energy input streams that run off steep granitic ridges during rain events and a relatively low energy output. The watershed is sparsely vegetated with high alpine trees and shrubs. Emerald Lake has a lesser lake to basin ratio than the other lakes that results in a greater indirect watershed input potential. Despite the steep sides the lake itself is shallow and flat-bottomed (Table 2; Figure 5).

3.2. Core collection

SCUBA divers collected three sediment cores from each of the four selected lakes. Push cores were taken except for Wildcat Lake; Wildcat Lake had what appeared to be a high sedimentation rate as evidenced by soft and compressible sediments. For Wildcat Lake a piston-pulley coring system was rigged to obtain a deep core. SCUBA collection usually allowed a visual assessment of surficial sediments and care was taken to minimize disturbance to lake sediments. Lake centers or flat shelves in approximately 10 m water depth were identified using bathymetry maps when available to minimize focusing of sediments. One core from each lake was extruded and sectioned in 0.3-0.5 cm increments using clean hand techniques, placed in double plastic bags, and stored at 4°C (USEPA, 1999). The remaining cores were maintained in an upright position to preserve the sediment-water interface and were placed in refrigerated storage for further analysis.

3.3. Atmospheric components

3.3.1. Lead-210 dating of lake sediments

Sediment and mass accumulation rates were determined from excess ^{210}Pb ($^{210}Pb_{ex}$), in a series of core samples, using the granddaughter proxy ^{210}Po measured by alpha spectrometry (Goldberg and Bruland, 1974; Lewis *et al.*, 2002). Lead-210 can be used for dating sediments that have been deposited during the last 120 years; Dates prior to 1880 were extrapolated from the measured deposition rates.

Polonium-210 and Hg were leached from a pre-weighed aliquot of wet sediment (3g) in a HCL, (Baker® reagent grade 12 N) : HNO_3 (Baker® reagent grade 16 N), 4:1 mL aqua-regia for 24 hours (Bloom, 1999). Samples were spiked with 2 mL of calibrated ^{208}Po + ^{209}Po yield tracer (^{208}Po activity = 6.015 dpm/g and ^{209}Po activity = 3.660 dpm/g; cal. 2/1/1997 to ± 2.5% (2 SE)). The sediment digestion volume was brought up to 40 mL volume with 4% HCl (Baker® reagent grade) using high purity de-ionized water (Milli-Q®). The remaining supernatant was pipetted into a 100 mL glass beaker and dried at 80°C. Nitrate salts were converted to chloride form by subsequent additions of approximately 100 μL HCl (6.0 N) followed by drying on low heat. To redissolve the sample in preparation for polonium autodeposition, 60 mL of 0.5 N HCl was added to the sample. To eliminate interference from Fe (III) during autodeposition, ascorbic acid (0.1 g) was added to reduce Fe (III) to Fe (II) (Flynn, 1968). Pure silver (Ag) disks were acid cleaned and mounted in magnetic Teflon® disk holders and placed in sample beakers. Autodeposition of ^{210}Po and the ^{208}Po + ^{209}Po yield tracer solution was achieved by heating the dissolved sample on a hot plate and stirring with the plating assembly for four hours at 80°C (Flynn, 1968). The Ag disks were each placed into an alpha-spectrometer (Tennelec TC 256) under a 450 mm^2 PIPS detector. Counts were collected with an Ortec® hardware/software system. Counting was continued until the total counts exceeded 1000 counts for the isotopic signal with the lowest yield, which resulted in a counting error of less than 3%.

The activity of ^{210}Pb was determined based on the ratio of counts relative to the known activity of the sample spike. The ^{210}Po activities were calculated using the known ^{208}Po spike activity and multiplied by the detected ^{210}Po: ^{208}Po ratio. It is necessary to assume that ^{210}Po was in equilibrium with ^{210}Pb and is likely an accurate assumption because of the sample depths (greater than 2 years of accumulation). Because of the close proximity of the ^{210}Po peak to the ^{208}Po peak, a tailing correction was applied (Figure 6; Fleer, 1984).

Sedimentation rates were calculated from $^{210}Pb_{ex}$ activities that decreased exponentially to supported activities in older sections of the sediment cores (Goldberg and Bruland, 1974). To calculate sedimentation rates, a regression was applied to the natural log of $^{210}Pb_{ex}$ activities versus sedimentation depth (Goldberg and Bruland, 1974); hence,

$$S = \frac{\lambda_{210}}{m},$$

where S represented the sedimentation rate in cm/yr, λ_{210} was the ^{210}Pb decay constant (ln(2)/22.26 yr), and m was the slope of the ln ($^{210}Pb_{ex}$/depth (cm); Goldberg and Bruland, 1974). Mass accumulation rate ($g\cdot cm^{-2}y^{-1}$) was calculated by multiplying the sedimentation rate ($cm\cdot yr^{-1}$) with density (g-dry wt.$\cdot cm^{-3}$).

3.3.2. Hg analysis

The ^{210}Pb dates were used to select approximately 20 increments from each core to represent pre- and post-industrial periods and analyzed for Hg_T. Sediments were previously digested for ^{210}Pb analysis and analyzed by a Perkin Elmer Flow Injection Hg System® (FIMS) 400 (Heim *et al.,* 2007). Sediments with mercury concentrations below the FIMS minimum detection limit (MDL) of 10.5 ng/g sediment dry wt. were analyzed by sodium borohydride reduction and cold vapor atomic fluorescence spectroscopy (CVAF) that has a MDL of 0.2 ng/L (Landing *et al.,* 1998; Bloom *et al.,* 1999). Relative percent difference (RPD) of duplicate digestions that indicate precision averaged 9.4 % (n=8 pairs). Matrix spikes that indicate matrix interference and accuracy averaged 110.2 % (n=8 pairs) recovery and RPD between spike duplicates averaged 7.7%. Standard reference material (SRM) that indicate accuracy averaged 108.2 % recovery. SRM included 1944 (National Institute of Standards and Technology (NIST) New York/ New Jersey waterway; 3.4 $mg{\cdot}kg^{-1}$ Hg^T) and 2709 (NIST) San Joaquin soil; 1.4 $mg{\cdot}kg^{-1}$ Hg^T). Additional on-going precision recovery (OPR) and matrix spikes that indicate precision and accuracy averaged 99.7 % (n=5) and 104.5% respectively, for the CVAFS analysis.

3.3.3. Modern atmospheric wet Hg deposition estimates

Modern atmospheric wet Hg deposition was estimated in three locations across California to determine regional variation using a modified Aerochem metrics atmospheric wet deposition collector (Landing *et al.,* 1998). Two of the collectors were located in Sacramento-San Joaquin Central Valley, one at Twitchell Island and the other at Woodland. The third collector was located at Point Reyes Bird Observatory (PRBO) on the coast near Wildcat Lake. Monthly samples were collected using clean hand techniques during 2003 to 2006 to obtain average annual wet depositions (USEPA, 1999). Samples were sent to Texas A & M University for analysis (Landing *et al.,* 1998).

3.3.4. Spatial correlation and Hg flux and mass loading calculations

Atmospheric and lake sediment Hg flux was calculated by multiplying the ^{210}Pb derived mass accumulation rates and Hg concentrations for each lake. Atmospheric, watershed, and lake mass loadings were calculated by multiplying the Hg flux and by each associated surface area. Lake to lake temporal Hg correlations were applied to further investigate the relative spatial contribution of global, regional, and local Hg sources to California.

3.4. Watershed components

3.4.1. Qualitative microscopy characterization

Initial characterization of the lake sediments was conducted by microscopy. Petrographic analysis of sediment smear slides were carried out at core depths characterized by prominent sedimentary features (e. g. lamination) and changes in sediment composition (Aiello and Kellett, 2006). Slides were observed under both parallel light to analyze the sediments for diatoms and amorphous organic debris and cross-polarized light to detect minerals. A photomicroscopy slide micrometer was used to estimate diatom and mineral sizes for particle size verification. The smear slides were observed to characterize the relative contribution of watershed and lake derived materials and to interpret the particle size data (see below).

3.4.2. Particle size interpolation

Particle size was measured using an LS 13 320 Beckman Coulter Inc.® particle size analyzer (Beckman methods PN 7222061 Rev. A). Methods were modified from Murray

(2002). Sediments were digested with 30% hydrogen peroxide to dissolve organics followed by a 10% Calgon® treatment. The interpolation software apportions the particles into size ranges that represent clays, diatoms, minerals, and other materials that were qualitatively verified by microscopic analysis (Aiello and Kellett, 2006).

3.4.3. Magnetic susceptibility

Magnetic susceptibility was measured using a MS2 Bartington® Magnetic Susceptibility Meter and a MS2K High Resolution Surface Scanning Sensor (Best *et al.*, 1996). The meter had a sensitivity of 2x10^{-6} SI (2x10^{-7} CGS). Sample material was placed within the influence of the low frequency, 100 ìT, alternating magnetic field produced by the sensor. Wet sediment samples were frozen to counteract the diamagnetic effect of water and measured through sample bags.

3.4.4. Organic carbon and nitrogen

Sediment samples were analyzed for organic composition by a Control Equipment Corp. 440 Elemental Analyzer (Exeter Analytical, Inc.) using a modified method from EPA MARPCPN I study (USEPA, 1992). Approximately 6 grams of wet sediment was oven dried at 60°F for 48 hours. Sediments were homogenized using a ball mill. Three replicates of each sample were dried, weighed to 0.01 g, and analyzed to calculate precision. Standard Reference Materials, cystine (National Institute of Standards and Technology) and BCSS-1 (National Research Council of Canada Marine Sediment), and blanks were run to verify instrument accuracy.

3.5. Atmospheric and Watershed Component Regression Analysis

Mercury concentrations and watershed component data was standardized and regressed to determine whether there was an association between Hg and watershed components that represent changes in lake sedimentation processes or episodic runoff events. A strong association would indicate that Hg concentrations in lake sediments were dependent on an alternative process other than atmospheric Hg deposition.

4. Results

4.1. Atmospheric components

4.1.1. Lead-210 dating in lake sediments

Lead-210 in each lake core decreased exponentially down core to supported ^{210}Pb activities (Figures 7 and 8). Lead-210 derived sedimentation rates for Wildcat Lake were greater than the alpine Castle, Island and Emerald Lakes, which had relatively slow sedimentation rates. A constant rate of ^{210}Pb supply (CRS) was assumed for each core (Robbins, 1978; Broecker and Peng, 1982; Appleby and Oldfield, 1992). Although ^{210}Pb was atmospherically deposited to each lake basin at a relatively constant rate, the mixed, hydrous sediments altered the density with core depth, which can be observed by the relatively constant $^{210}Pb_{ex}$ towards the top of each core. The top, approximately 10-15 cm of each dated core, consisted of a flocculent, hydrous mixed layer. Determining the endpoints of the mixed layer and the $^{210}Pb_{ex}$ during slope analysis was difficult and resulted in some uncertainty, as a result sedimentation rates were calculated by both including and excluding the mixed layer to estimate the associated error (Figure 9). Density changes were accounted for by referring to mass accumulation rates for mass loading calculations.

4.1.2. Hg analysis

Each lake site demonstrated a modern elevation in atmospheric Hg_T concentration (modern concentrations ranged from 99-182 ppb) above natural baseline levels (historic concentrations ranged from 5-39 ppb; Figure 10; Table 3). The greatest to least enrichment in Hg_T concentrations since 1850 among lakes occurred in Castle (14 to 143 ppb; averaged past and modern [Hg_T] respectively), Emerald (22 to 107 ppb), Island (32 to 122 ppb), and Wildcat Lakes (46 to 92 ppb).

4.1.3. Spatial correlation and Hg flux and mass loading calculations

An elevation above pre-anthropogenic (before 1850) sediment Hg concentrations was observed in Wildcat Lake (factor of 2 = 2x), Castle Lake (10x), Island Lake (4x), and Emerald Lake (5x; Table 3). Wildcat Lake had the greatest Hg flux to lake sediments followed by Castle, Emerald and Island Lakes, consecutively. The estimated watershed atmospheric Hg mass loadings to Wildcat Lake (8.7×10^3 $\mu g \cdot yr^{-1}$), Castle Lake (9.8×10^4 $\mu g \cdot yr^{-1}$), Island Lake (6.1×10^4 $\mu g \cdot yr^{-1}$), and Emerald Lake (9.6×10^3 $\mu g \cdot yr^{-1}$) were estimated from atmospheric Hg wet deposition flux and watershed area and compared to modern lake mass Hg loadings (Table 4). The global Hg source lake (Wildcat) had the strongest spatial correlation to the regional Hg belt lake (Castle) and the regional mine source Lake (Island; Table 5). The Hg source lake (Castle) exhibited the strongest correlation to the regional mine source lake (Island) and the regional background lake (Emerald).

4.2. Watershed components

4.2.1. Qualitative microscopy characterization

Sediments were mainly composed of diatoms and fecal pellets from zooplankton (e. g. rotifers and *Daphnia*) except during periods where increases in grain size and other terrigenous materials (e. g. silt-sized quartz and feldspar minerals) and fibrous twigs, leaves, and pollen were evident. A qualitative microscopic analysis of the sediment revealed that particle size ranges largely represented the following compositions among lakes: <50 μm = centric and pennate diatoms, 51-200 μm = fecal pellets, amorphous organic debris and terrigenous grains. Grain size variability was very low in Wildcat Lake, compared to the watersheds of Castle and Emerald Lakes. Wildcat sediment mainly consisted of diatoms and organic debris (flocculent organic material that may have originated from either lake or watershed sources). Castle Lake had the most defined laminations and extreme episodic variability. Island Lake was relatively homogenous with the exception of one layer of organic debris comprised of twigs and sand. Emerald lake had episodic variability in grain size, comparable to Castle Lake. All lakes contained amorphous organic debris that was difficult to discern between lake or watershed sources and contained very few minerals (Figure 11).

4.2.2. Particle size interpolation

Particle size measurements confirmed the smear slide analysis. Episodic increases in grain size occurred in both Castle Lake and Emerald Lake while Wildcat and Island were more homogenous with slight increases (Figure 12). A greater percent volume particle size remained under <50 μm except during high-energy depositional events where a greater percent volume of particles were between 51-200 μm and above (terrigenous material composed mainly of large grains).

4.2.3. Magnetic susceptibility

Magnetic susceptibility corresponded with the increases in particle size during high-energy depositional events in Castle and Emerald Lakes (Figure 13). The homogenous organic-rich lakes, Wildcat and Island, demonstrated minimal variability in magnetic susceptibility while the more granitic, higher altitude lakes, Emerald and Castle, demonstrated episodic elevations in magnetic susceptibility above the average background values, which may correspond to input of mineral-rich terrigenous material during storm events. Sand laminations containing highly magnetic minerals deposited during storm events were detected in Emerald and Castle Lakes.

4.2.4. Organic carbon and nitrogen

POC/PON concentrations were relatively constant in Island (range 11-16 POC %Wt.) and Emerald Lakes (5-9 POC %Wt.). Wildcat (8-25 POC %Wt.) and Castle Lakes (4-21 POC %Wt.), however, demonstrated an increase in POC in the top 20-30 cm (Figure 14).

4.3. Atmospheric and Watershed Component Regression Analysis

Regressional analysis between Hg concentrations and watershed components revealed that organic nitrogen content (r^2=0.574), organic carbon content (r^2=0.434), and magnetic susceptibility (r^2=0.001) demonstrated a positive relationship with Hg while particle size (r^2=0.012) exhibited a negative relationship with Hg (Figure 15).

5. Discussion

5.1. Spatial and temporal trends of atmospheric Hg deposition in California

Wildcat, Castle, Island, and Emerald Lakes all demonstrated elevated Hg concentrations post 1850 (Table 3 and 4; Figure 10). Wildcat Lake, the coastal site chosen to represent global Hg input, exhibited the lowest increase in sediment Hg concentration, 2x greater than pre-1850 Hg concentrations, and greatest annual flux of Hg to sediments. Castle Lake, the coast range site chosen to represent the geologic mercury belt and mine input, revealed the greatest increase in sediment Hg concentrations at 10x greater since 1850. This provides evidence for local and regional Coast Range Hg belt contributions and abandoned mine input. Island Lake, the site chosen to represent regional abandoned gold mine aerosol Hg input, exhibited more elevated Hg concentrations than Wildcat at 4x greater than 1850, and provides evidence for local and regional gold mine inputs from atmospheric sources. Emerald Lake, the site chosen to represent regional background input excluding gold and Hg mines, revealed an increase in Hg similar to Island Lake at 5x greater than 1850. Because there were no other regional sources, the Hg increase in this high alpine lake provides evidence for atmospheric input from municipal and industrial Hg emissions. The sources for these lakes have been inferred from the geographical locations, local wind trajectories, and spatial correlations given that there remain no proxy that would enable definitive attributions of source.

The spatial correlations indicate a strong association between the global source reference (Wildcat Lake) to Castle and Island Lakes, which support that a portion of the Hg is of global origin. The regional geologic Hg source lake (Castle) was strongly correlated with the Au mine source lake (Island), which provides evidence for additional sources to the global input from mining emissions.

It has been well documented that the global pool of atmospheric Hg has increased by a factor of 2-3 (since 1850) and may dominate Hg spatial deposition uniformly (Rada *et al.*, 1989; Schuster *et al.*, 2002; Fitzgerald *et al.*, 2005). Nater and Grigal (1992) conducted a study to determine the spatial variability of Hg deposition in Minnesota along transects radiating from point sources and found that regional sources contribute substantially to the local Hg pool relative to the global signal. Mason *et al.* (2000) found that urban site wet deposition fluxes were 2-3 times greater than rural sites. The evidence from this study supports the proposal that California is subjected both to global and regional Hg inputs, as was inferred from the remote alpine lake Hg profiles.

5.2. Watershed components and mass loading

To make informed management decisions, water and air quality regulators require information on atmospherically deposited Hg on land and how much gets washed into aquatic systems. Atmospherically deposited Hg is thought to be strongly retained in watersheds because it binds to organic material (Mason *et al.,* 2000). Due to the complex nature of Hg cycling, researchers remain uncertain how much Hg runoff is introduced to aquatic systems (e.g. Lindberg and Turner, 1988; Hintelmann *et al.,* 2002).

The Mercury Experiment To Assess Atmospheric Loading In Canada and the United States (METAALICUS) study made an attempt to discern the contribution of different pathways by depositing a known amount of Hg tracer in a watershed and tracking its diffusion into the environment (Hintelmann *et al.,* 2002). The result was that less than 1% was transported by runoff, 66% remained in or on vegetation, and the remainder was bound to soils; however, METAALICUS researchers estimated approximately 20% of the ambient lake sediment Hg originated from the watershed, indicating that Hg may have a long residence time in the watershed before it reaches lake sediments. Thus, in some lake basins, the timescale of Hg preservation in sediments may be reduced and may record phase lags for specific watershed deposition events.

Watershed component analyses including microscopy smear slides, particle size, magnetic susceptibility, and particulate organic carbon and nitrogen were conducted to estimate watershed runoff contribution to lake sediment Hg levels and support atmospheric Hg deposition as the major source of Hg to lake sediments. Because of the low basin relief and subsequent low-energy runoff coefficients, Wildcat and Island Lake sediments were relatively homogenous down core with respect to watershed markers making it difficult to discern laminations. Castle and Emerald Lakes, however, had more prominent sedimentary structures that represented large storms, fires, and other events as a result of the steeper sloped basins and subsequent high energy depositional events. A regression between each of the watershed components and Hg was applied to further investigate whether Hg variability was influenced by additional processes other than atmospheric Hg deposition. Mercury concentrations had the strongest relationship to organic nitrogen content (positive; r^2=0.574) and organic carbon content (positive; r^2=0.434). The relationship between Hg and the remaining watershed components including particle size (negative; r^2=0.012) and magnetic susceptibility (positive; r^2=0.001) was not significant. This implies that Hg concentrations in sediments are not strongly influenced by runoff coefficients, as inferred from the weak associations between Hg and runoff components (magnetic susceptibility and particle size). It is difficult to confirm whether the relationship between Hg and organic components is independent or if Hg sedimentation efficiency is dependent on lake productivity. The relationship between Hg and organic components is not consistent among lakes suggesting a weaker association than atmospheric Hg deposition. It is more likely that organic matter is responsible for small-scale variability while atmospheric Hg deposition is driving the overall increase in Hg sedimentation over time.

Sediments are unevenly deposited to lake bottoms therefore one core may not accurately represent the mass loading for the entire lake basin (Davis and Ford, 1982). In general, more sediment accumulates in the middle of lakes. In this study we attempted to minimize sediment-focusing effects by sampling lakes with relatively shallow, flat bottoms and relatively small areas. Atmospheric wet deposition mass loading for each lake was calculated using the regional wet atmospheric Hg flux to apportion how much of the lake sediment Hg originated from direct atmospheric wet deposition. The calculated contribution of direct atmospheric deposition to lake sediments was relatively small (Wildcat 2%, Castle 8%, Island 31%, and Emerald 6%) contrary to the watershed component analysis that indicated atmospheric deposition as the major source of Hg. There is minimal evidence obtained from watershed component analyses that indirect wet atmospheric Hg deposition (runoff) is a major contributor to lake sediments, however, the potential Hg deposited on Wildcat, Castle, Island and Emerald watershed soils equals 18%, 34%, 34%, and 38% of the lake sediment Hg, respectively. The mass loading calculations implies an additional source of Hg other than direct and indirect atmospheric wet deposition. If the potential indirect wet atmospheric Hg contribution is integrated to lake sediments there remains an additional source of Hg to Wildcat (80%), Castle (58%), Island (35%) and Emerald Lakes (56%).

A partial explanation for the discrepancy in the Hg sediment budget is that modern atmospheric Hg deposition for California is underestimated (Table 6). The Aerochem collectors monitor wet Hg deposition only, and are not designed to collect dry Hg deposition or Hg associated with fog. Dry deposition is difficult to collect and currently there are no measurements in California to assess the importance of this contribution. Atmospheric deposition models estimate that dry deposition of mercury, depending on location, can be from 0.25 to 3 times the rate of wet deposition (Seigneur *et al.,* 2004). It may be that Wildcat receives additional Hg deposition from coastal aerosols and fog that are not measured by the Aerochem wet deposition collector. Castle Lake may receive significant amounts of dry Hg deposition from surrounding exposed HgS deposits or regional volcanic activity originating from Mt. Shasta or Mt. Lassen.

5.3. Biotic impacts of atmospheric Hg deposition to aquatic systems

Many studies have identified atmospherically derived Hg as the major source to remote lakes (e.g. Morel *et al.*, 1998; Schwesig *et al.*, 1999; Mason *et al.*, 2000; Vaidya *et al.*, 2000). Atmospherically derived Hg is mainly deposited in its ionic form Hg (II), which is an important Hg source for methylation in aquatic systems (Mason *et al.*, 2000). Hg (II) is readily methylated (MeHg; MMHg and DMHg) and subsequently bioaccumulated up the food chain (Morel *et al.*, 1998; French *et al.*, 1999; Schwesig *et al.*, 1999). Fish, birds, and other associated aquatic biota experience a wide range of physiological, reproductive and biochemical negative effects as a response to organic and inorganic Hg toxicity (Boening, 2000). Fish are particularly susceptible to accumulating elevated levels of Hg because of their upper trophic level and comparatively long life spans (Trudel and Rasmussen, 2001; Uryu *et al.*, 2001).

Several studies have attempted to define a relationship between ambient inorganic Hg and MeHg concentrations in aquatic environments and have found weak correlations except in locations with direct-point source contaminations such as gold mine tailings. A mesocosm study by Kimball (2006) demonstrated a strong correlation between Hg (II) and Hg methylation rates and a weak correlation between Hg^0 and Hg methylation rates thus a greater flux of Hg (II) is expected to result in greater production of Mono Methyl Hg (MMHg). A national pilot study was conducted by Krabbenhoft *et al.* (1999) in an attempt to determine the main contributing factors to MeHg production. They found little evidence to support MeHg production associated with elevated inorganic Hg concentrations suggesting that inorganic Hg is not the limiting factor in most aquatic environments. Meanwhile, Hammerschmidt and Fitzgerald (2005) found a spatial correlation between mosquito MMHg concentrations and atmospheric Hg deposition among locations where atmospheric deposition, which is mainly comprised of Hg (II), was the principal source. Furthermore, Hammerschmidt and Fitzgerald (2006) demonstrated a strong spatial correlation between Large Mouth Bass MMHg concentrations and atmospheric Hg deposition. Hrabik and Watras (2002) conducted a study in Little Rock Lake in northern Wisconsin where atmospheric Hg deposition has decreased regionally as a result of improved emission regulations and found that fish Hg concentrations have also decreased during the last decade. Overall, recent studies support atmospheric Hg deposition as a major source of bioavailable Hg to aquatic systems (Johnson *et al.,* 1987). Therefore, lake sediment Hg concentrations that represent atmospheric Hg trends can be used to infer trends in biotic exposure. Historic biotic exposure, if scaled linearly to deposition, would therefore have been 2 (coastal; global), 5 (central; regional), to 10 (coast range; local Hg source) times less than present day concentrations prior to the industrial revolution and the California gold rush.

6. Summary and Conclusions

Historic lake sediments provide critical information on past Hg concentrations in the natural environment prior to anthropogenic industrial activities. This is the first study conducted in California that attempts to determine both spatial and temporal variability. It is necessary to identify atmospheric Hg sources in California in order to ascertain the effectiveness of regional air emission regulations, which would have little effect if atmospheric deposition originated from global sources. This study suggests regional Hg sources from industrial emissions and historic gold and Hg mines are contributing to the overall atmospheric Hg deposition budget of California in addition to the global input. Therefore, local and regional regulation caps on industrial emissions and remediation of abandoned mines would decrease the amount of Hg entering aquatic systems in California.

The hydrous nature of lake sediments (85-95% moisture) is comparable to particulate Hg concentrations in rivers and estuaries. The modern, surficial lake sediment concentrations are comparable to those found in water bodies through out the central valley (Table 7). This suggests that the elevation in lake sediment Hg concentrations from pre-anthropogenic levels of the study lakes located in the upper watersheds of the Sacramento and San Joaquin River systems may be extrapolated throughout California water bodies.

7. References

Aiello, I. W., Kellett, K., 2006. Sedimentology of open-ocean biogenic sediments from ODP leg 201, Eastern Equatorial Pacific (sites 1225 and 1226). In: Jørgensen, B. B., D'Hondt S. L., and Miller, D. J. (Eds.), Proc. ODP, Sci. Results, 201: WWW, pp. 1-25.

Alpers, C. N., Hunerlach, M. P., May, J. T., Hothem, R. L., Taylor, H. E., Antweiler, R. C., De Wild, J. F., Lawler, D. A, 2004. Geochemical characterization of water, sediment, and biota affected by mercury contamination and acidic drainage from historical gold mining, Greenhorn Creek, Nevada County, California, 1999-2001. US Geol. Surv. Open-File Report, 2004-5251, 278.

Appleby, P. G., Oldfield, F., 1992. Application of lead-210 to sedimentation studies. In: Ivanovich, M., Harmon, R. S. (Eds.), Uranium-series disequilibrium: Applications to earth, marine, and environmental sciences. Claredon Press, Oxford, pp. 731-778.

Best, P. J., Reynolds, R. L., Rosenbaum, J. G., Drexler, J., Adam, D. P., 1996. Sediment magnetic, paleomagnetic, and geochemical data from lacustrine sediment in a core from Grass Lake, Siskiyou County, California. US Geol. Surv., Open-File Report 96-294.

Bilali, L. El, Rasmussen, P. E., Hall, G. E. M., Fortin, D., 2002. Role of sediment composition in trace metal distribution in lake sediments. Appl. Geochem., 17, 1171-1181.

Bindler, R., Renberg, I., Appleby P.G., Anderson, N. J., Rose, N.L., 2001. Mercury accumulation rates and spatial patterns in lake sediment from West Greenland: a coast to margin transect. Environ. Sci. Technol., 35, 1736-1741.

Bloom, N. S., Gill, G. A., Cappellino, S., Dobbs, C., McShea, L., Driscoll, C., Mason, R., Rudd, J., 1999. Speciation and cycling of mercury in Lavaca Bay, Texas sediments. Environ. Sci. Technol., 33, 7-13.

Boening, D. W., 2000. Ecological effects, transport, and fate of mercury: a general review. Chemosphere, 40, 1335-1351.

Broeker, W. S., Peng, T. H., 1982. Tracers in the Sea. The Lamont-Doherty Geological Observatory, Columbia University, Palisades, New York, 253-274.

Churchill, R. K. and Clinkenbeard, J. P, 2003. An assessment of ecological and human health impacts of mercury in the bay-delta watershed. CALFED final project task 5c1: assessment of the feasibility of remediation of mercury mine sources in the cache creek watershed. California Department of Conservation, California Geol. Surv.

Coolbaugh, M. F., Gustin, M. S., Rytuba, J. J., 2002. Annual emissions of mercury to the atmosphere from natural sources in Nevada and California. Environ. Geol., 42, 338-349.

Davis, M. B., Ford, M. S., 1982. Sediment focusing in Mirror Lake, New Hampshire. Limnol. Oceanogr., 27(1), 137-150.

Fitzgerald, W. F., Engstrom, D. R., Mason, R. P., Nater, E. D., 1998. Critical Review: The Case for Atmospheric Mercury Contamination in Remote Areas. Environ. Sci. Technol. 32(1), 1-7.

Fitzgerald, W. G., Engstrom, D. R., Lamborg, C. H., Tseng, C., Balcom, P. H., Hammershmidt, C. R., 2005. Modern and historic atmospheric mercury fluxes in Northern Alaska: Global sources and arctic depletion. Environ. Sci. Technol., 39, 557-568.

Fleer, A. P., Bacon, M. P., 1984. ^{210}Po tailing correction method. Nuclear Instruments and Methods in Physics Research, 223, 243-249.

Flynn, W. W., 1968. The determination of low levels of polonium-210 in environmental materials. Anal. Chim. Acta., 43, 221-227.

French, K. J., Scruton, D. A., Anderson, M. R., Schneider, D. C., 1999. Influence of Physical and Chemical Characteristics on Mercury in Aquatic Sediments. Water Air Soil Pollut., 110, 347-362.

Goldberg, E.D., Bruland, K., 1974. Radioactive geochronologies. In: The Sea: Marine Chemistry, 5, Goldberg, E. D. (Ed.), John Wiley and Sons, New York, pp. 456-489.

Gustin, M.S., 2003. Are mercury emissions from geologic sources significant? A status report. Sci. Total Environ., 304, 153-167.

Hammerschmidt, C. R., Fitzgerald, W. F., 2005. Methylmercury in mosquitoes related to atmospheric deposition and contamination. Environ. Sci. Technol., 39, 3034-3039.

Hammerschmidt, C. R., Fitzgerald, W. F., 2006. Methylmercury in freshwater fish linked to atmospheric mercury deposition. Environ. Sci. Technol., 40, 7764-7770.

Harnly, M., Seidel, S., Rojas, P., Fornes, R., Flessel, P., Smith, D., Kreutzer, R., Goldman, L., 1997. Biological monitoring for mercury a community with soil and fish contamination. Environ. Health Perspect., 105, 424-429.

Hayes, T. P., Kinney, J. Jr., Wheeler, N. J. M. 1984. California Surface Wind Climatology. California Air Resources Board (CARB), Aeromatic Data Division, 1-73.

Heyvaert, A. C., Reuter, J. E., Slotton, D. G., Goldman, C. R., 2000. Paleolimnological reconstruction of historical atmospheric lead and mercury deposition at Lake Tahoe, California-Nevada. Environ. Sci. Technol., 34, 3588-3597.

Heim, W. H., Coale, K. H., Stephenson, M., Choe, K., Gill, G. A., Foe, C., 2007. Spatial and habitat-based variations in total and methyl mercury concentrations in surficial sediments in the San Francisco Bay-Delta. Environ. Sci. Technol., in press.

Hintelmann, H., Harris, R., Heyes, A., Hurley, J. P., Kelly, C. A., Krabbenhoft, D. P., Lindberg, S., Rudd, J. W. M., Scott, K. J., St. Louis, V. L., 2002. Reactivity and mobility of new and old mercury deposition in a boreal forest ecosystem during the first year of the METAALICUS study. Environ. Sci. Technol., 36, 5034-5040.

Hornberger, M. I.; Luoma, S. N.; van Geen, A.; Fuller, C.; Anima, R., 1999. Historical trends of metals in the sediments of San Francisco Bay, California. Mar. Chem., 64, 39-55.

Hrabik, T. R., Watras, C. J., 2002. Recent declines in mercury concentrations in a freshwater fishery: isolating the effects of de-acidification and decreased atmospheric mercury deposition in Little Rock Lake. Sci. Total Environ., 297, 229-237.

Johnson, M. G., Culp, L. R., George, S. E., 1986. Temporal and spatial trends in metal loadings to sediments of the Turkey Lakes, Ontario. Can. J. Fish. Aquat. *Sci.*, 43, 754-762.

Johnson, M. G., 1987. Trace element loadings to sediments of fourteen Ontario lakes and correlations with concentration in fish. Can. J. Fish. Aquat. Sci., 44, 3-13.

Kimball, T., 2006. Mercury methylation in sediments from coastal and Sierra watersheds: Implications for methylmercury mitigation in the San Francisco Bay-Delta complex. Masters Thesis - California State Monterey Bay.

Krabbenhoft, D. P., Wiener, J. G., Brumbaugh, W. G., Olson, M. L., Dewild, J. F., Sabin, T. J., 1999. A National Pilot Study of Mercury Contamination of Aquatic Ecosystems along Multiple Gradients, Morganwalp, D.W., and Buxton, H.T., (Eds.), 1999, U.S. Geological Survey Toxic Substances Hydrology Program--Proceedings of the Technical Meeting, Charleston, South Carolina, March 8-12, 1999--Volume 2--Contamination of Hydrologic Systems and Related Ecosystems: U.S. Geological Survey Water-Resources Investigations Report 99-4018B, pp. 147-160.

Landing, W. M., Guentzel, J. L., Perry, J. J. Jr., Gill, G. A., Pollman, C. D., 1998. Methods for measuring mercury and other trace species in rainfall and aerosols in Florida. Atmos. Environ., 32, 909-918.

Lent, R. M., Alexander, C. R., 1997. Mercury accumulation in Devils Lake, North Dakota - effects of environmental variation in closed-basin lakes on mercury chronologies. Water Air Soil Pollut., 98, 275-296.

Lewis, R. C., Coale, K. H., Edwards, B. D., Marot, M., Douglas, J. N., Burton, E. J., 2002. Accumulation rate and mixing of shelf sediments in the Monterey Bay National Marine Sanctuary. Mar. Geol., 181, 157-169.

Lindberg, S. E., Turner, R. R., 1988. Factors influencing atmospheric deposition, stream export, and landscape accumulation of trace metals in forested watershed. Water Air Soil Pollut., 39 (1-2), 123-156.

Lockhart, W. L., Wilkinson, P., Billeck, B. N., Danell, R. A., Hunt, R. V., Brunskill, G. J., Delaronde, J., St. Louis, V., 1998. Fluxes of mercury to lake sediments in central and northern Canada inferred from dated sediment cores. Biogeochemistry, 40, 163-17.

Lucotte, M., Mucci, A., Hillaire-Marcel, C., Pichet, P., Grondin, A., 1995. Anthropogenic mercury enrichment in remote lakes of Northern Quěbec (Canada). Water Air Soil Pollut., 80, 467-476.

Marchetto, A., Mosello, R., Rogora, M., Manca, M., Boggero, A., Morabito, G., Musazzi, S., Tartari, G. A., Nocentini, A. M., Pugnetti, A., Bettinetti, R., Panzani, P., Armiraglio, M., Cammarano, P., Lami, A., 2004. The chemical and biological response of two remote mountain lakes in the Southern Central Alps (Italy) to twenty years of changing physical and chemical climate. J. Limnol. 63(1), 77-89.

Mason, R. P., Fitzgerald, W. F., Morel, F. M. M., 1994. The biogeochemical cycling of elemental mercury: Anthropogenic influences, Geochim. Cosmochim. Acta, 58(15), 3191-3198.

Mason, R.P., Lawson, N.M., Sheu, G.R., 2000. Annual and seasonal trends in mercury deposition in Maryland. Atmospheric Environment, 34, 1691-1701.

May, J. T., Hothem, R. L., Alpers, C. N., Law, M. A., 2000. Mercury bioaccumulation in fish in a region affected by historic gold mining: The South Yuba River, Deer Creek, and Bear River watersheds, California. U. S. Geol. Surv. Open-File Report, 00-367, 30.

Mercury deposition network (MDN), 2005. National Atmospheric Deposition Program. http://nadp.sws.uiuc.edu/mdn/.

Morel, F. M., Kraepiel, A. M., Amyot, M., 1998. The chemical cycle and bioaccumulation of mercury. Annual Reviews of Ecological Systems, 29, 543-66.

Murray, M. R., 2002. Is laser particle size determination possible for carbonate-rich lake sediments? J. of Paleolimnol., 27, 173-183.

Nacht, D. M., Gustin, M. S., Engle, M. A., Zehner, R. E., Giglini, A. D., 2004. Atmospheric mercury emissions and speciation at the Sulphur Bank mercury mine superfund site, Northern California. Environ. Sci. Technol., 38, 1977-1983.

Nater, E. A., Grigal, D. F., 1992. Regional trends in mercury distribution across the Great Lakes states, north central USA. Nature, 358, 139-141.

Rada, R. G., Wiener, J. G., Winfrey, M. R., Powell, D. E., 1989. Recent increases in atmospheric deposition of mercury to North-Central Wisconsin lakes inferred from sediment analyses. Arch. Environ. Contam. Toxicol., 18, 175-181.

Robbins, J. A., 1978. Geochemical and geophysical applications of radioactive lead isotopes. In: J. P. Nriago (Ed.), Biogeochemistry of Lead: Elsevier, pp. 285-393.

Scholz, C. A., King, J. W., Ellis, G. S., Swart, P. K., Stager, J. C., Colman, S. M., 2003. Paleolimnology of Lake Tanganyika, East Africa, over the past 100 k yr. J. of Paleolimnol., 30, 139-150.

Schuster, P. F., Krabbenhoft, D. P., Naftz, D. L., Dewayne Cecil, L., Olson, M. L., Dewild, J. R., Susong, D. D., Green, J. R., Abbott, M. L., 2002. Atmospheric mercury deposition during the last 270 years: A glacial ice core record of natural and anthropogenic sources. Environ. Sci. Technol., 36, 2303-2310.

Schwesig, D., Ilgen, G., Matzner, E., 1999. Mercury and methylmercury in upland and wetland acid forest soils of a watershed in ne-bavaria, Germany. Water Air Soil Pollut., 113, 141-154.

Seigneur, C., Vijayaraghavan, K., Lohman, K., Karamchandani, P., Scott, C., 2004. Global source attribution for mercury deposition in the United States, Environ. Sci. Technol., 38, 555-569.

Slowey, A. J., Rytuba, J. J., Brown, G. E. Jr., 2005. Speciation of mercury and mode of transport from placer gold mine tailings. Environ. Sci. Technol., 39, 1547-1554.

Steding, D. J., Flegal, A. R., 2002. Mercury concentrations in coastal California precipitation: Evidence of local and trans-Pacific fluxes of mercury to North America. J. Geophys. Res. (Atmospheres), 107, D24, ACH 11-1.

Stevenson, J., Dodson, J. R., Prosser, I. P., 2001. A late quaternary record of environmental change and human impact from New Caledonia. Palaeogeogr., Palaeocl., Palaeoecol., 168, 97-123.

Suchanek, T. H., Richerson, P. G., Mullen, L. H., Brister, L. L., Becker, J. C., Maxon, A., Slotton, D.G., 1997. Interim final report: the role of the Sulphur Bank Mercury Mine site (and associated hydrogeological processes) in the dynamics of mercury transport and bioaccumulation within the Clear Lake Aquatic Ecosystem. Report to the United States Environmental Protection Agency Superfund Program, Region IX. Department of Environmental Science and Policy, University of California, Davis, CA.

Trudel, M., Rasmussen, J. B., 2001. Predicting mercury concentration in fish using mass balance models. Ecolog. App., 517-529.

Tseng, C. M., Lamborg, C., Fitzgerald, W. F., Engstrom, D. R., 2004. Cycling of dissolved elemental mercury in Arctic Alaskan lakes. Geochim. Cosmochim. Acta, 68, 1173-1184.

Uryu, Y., Malm, O., Thornton, I., Payne, I., Cleary, D., 2001. Mercury contamination of fish and its implications for other wildlife of the Tapajós Basin, Brazilian Amazon. Cons. Biol., 15, 438-446.

U. S. Environmental Protection Agency (USEPA), 1992. The analysis of carbon and nitrogen from sediments and the particulate fraction of water from estuarine/coastal systems using elemental analysis. Method MARPCPN I. University of Maryland System for Environmental and Estuarine Studies, Chesapeake Biological Laboratory. Revision 1.1. Environmental Monitoring Systems Laboratory, Office of Research and Development.

U. S. Environmental Protection Agency (USEPA), 1997. Mercury study: Report to Congress. Office of Air Quality Planning and Standards. Office of Research and Development. Washington, D.C., EPA-452/R-97-003.

U. S. Environmental Protection Agency (USEPA), 1999. Method 1669. Method for sampling ambient water for the determination of metals at EPA ambient criteria levels; Office of Water, Office of Science and Technology, Engineering and Analysis Division (4303), Washington, DC.

U. S. Environmental Protection Agency (USEPA), 2005. Proceedings and summary report: Workshop on the fate, transport, and transformation of mercury in aquatic and terrestrial systems. CLARIT Web Print, 625R02005.

Vaidya, O. C., Howell, G. D., Leger, D. A., 2000. Evaluation of the distribution of mercury in lakes in Nova Scotia and Newfoundland (Canada). Water Air Soil Pollut., 117, 353-369.

Wang, Q., Shen, W., Ma, Z., 2000. Estimation of mercury emission from Coal combustion in China. Environ. Sci. and Technol., 34, 2711-2713.

Wheatley, M., 1997. Social and cultural impacts of mercury pollution on aboriginal peoples in Canada. Water Air Soil Pollut., 97, 85-90.

Weiss-Penzias, P., Jaffe, D. A., Swartzendruber, P., Dennison, J. B., Chand, D., Hafner, W., Prestbo, E., 2000. Observations of Asian air pollution in the free troposphere at Mount Bachelor Observatory during the spring of 2004. J. Geophys. Res., 111, 1-15.

Western Regional Climate Center (WRCC), 2001. Historic Climate Information: Climate of California. http://www.wrcc.dri.edu.htm, accessed 2005.

Yang, H., Rose, N. L., Battarbee, R. W., 2002. Mercury and lead budgets for Lochnagar, a Scottish mountain lake and its catchment. Environ. Sci. Technol., 36, 1383-1388.

Table 1. A summary of studies that investigate historic and modern Hg concentrations using lake cores.

Authors	Location	Historic [Hg_T] Lake Sediment pre 1850 (ppb)	Modern [Hg_T] Lake Sediment post 1850 (ppb)	Modern [Hg_T] Enrichment	Notes
Rada *et al.*, 1989	Wisconsin	50	170	2	*n = 11 lakes*
Lent *et al.*, 1997	Dakota Lake, Dakota	53	265	2	*n = 4 lakes*
Lockhart *et al.*, 1998	Canada	50	80	1	*n = 18 lakes*
Hornberger *et al.*, 1999	San Fransisco Bay, CA	20	400	19	*mine tailings*
Heyvaert *et al.*, 2000	Lake Tahoe, CA	30	200	6	
Bindler *et al.*, 2001	Greenland	70	135	2	
Suchanek *et al.*, 1997	Clear Lake, CA	-	-	26	*mine tailings*
Yang *et al.*, 2002	Lochnagar, Scotland	50	200	3	
Fitzgerald *et al.*, 2005	Alaska	30	83	2	

Table 2. Limnologic characteristics of the studied lakes. Rainfall data courtesy of the Western Regional Climate Center (2001). Vegetative cover estimated from aerial photos.

Characteristics	**Wildcat Lake** Global Source	**Castle Lake** Regional Hg Belt Source	**Island Lake** Regional Mine Source	**Emerald Lake** Regional Background
Location	Pt. Reyes Coast	Trinity Mountains	Northern Sierra-Nevadas	Southern Sierra-Nevadas
GPS coordinates	37°58'5.35" N 122°47'8.49" W	41°13'38.61" N 122°22'54.91" W	39°23'56.17" N 122°47'8.49" W	36°35'49.52" N 118°40'49.66" W
Elevation (m)	61	1,676	2,103	2,835
Lake area (m^2)	3,096	23,392	15,136	2,408
Basin area (m^2)	38,528	102,168	16,856	163,400
Lake/ basin (%)	8%	23%	90%	1%
Maximum depth (m)	9	35	unknown	10
Core collection depth (m)	9	10	12	10
Vegetative cover	100%	80%	40%	15%
Annual precipitation (cm)	100-150	150-200	150-200	100-150

Table 3. Final modern and historic lake sediment Hg_T concentrations (ppb) and anthropogenic enrichment factors. Modern and historic averages were obtained from approximately five surficial and post 1850 concentrations.

Lake Atmospheric Source	**Average Modern Hg_T (ppb)**	**Average Historic Hg_T (ppb)**	**Maximum Hg_T (ppb)**	**Minimum Hg_T (ppb)**	**Anthropogenic Hg Enrichment**
Wildcat Lake Global	92 ± 12 (n=5)	46 ± 7 (n=5)	99	39	2
Castle Lake Regional Hg belt	143 ± 14 (n=5)	14 ± 6 (n=5)	176	5	10
Island Lake Regional mining	122 ± 2 (n=4)	32 ± 8 (n=5)	182	23	4
Emerald Lake Regional background	107 ± 20 (n=5)	22 ± 6.3 (n=3)	153	16	5

Table 4. Final Hg_T fluxes and mass loadings for the studied lakes. Modern wet deposition for Wildcat Lake was estimated from this study, Castle Lake wet deposition was estimated from the MDN Covelo site (CA97) while Island and Emerald Lake wet deposition was estimated from the California average atmospheric Hg deposition reported by Steding and Flegal (2002).

Description	**Wildcat Lake** Global Source	**Castle Lake** Regional Hg Belt Source	**Island Lake** Regional Mine Source	**Emerald Lake** Regional Background
Sedimentation rate ($cm \cdot yr^{-1}$)	0.559 ± 0.048	0.294 ± 0.005	0.131 ± 0.067	0.302 ± 0.040
Mass accumulation rate ($g \cdot cm^{-2} \cdot yr^{-1}$)	0.214 ± 0.042	0.038 ± 0.001	0.011 ± 0.001	0.067 ± 0.012
Modern lake sediment Hg_T flux ($\mu g \cdot m^{-2} \cdot yr^{-1}$)	197	54	13	71
Historic lake sediment Hg_T flux ($\mu g \cdot m^{-2} \cdot yr^{-1}$)	98	5	4	15
Modern wet Hg_T deposition ($\mu g \cdot m^{-2} \cdot yr^{-1}$)	2.8	4.2	4.0	4.0
Historic wet Hg_T deposition ($\mu g \cdot m^{-2} \cdot yr^{-1}$)	1.4	0.4	1.0	0.8
Wet Hg_T deposition to lake ($g \cdot yr^{-1}$)	0.009	0.098	0.061	0.010
Wet Hg_T deposition to basin ($g \cdot yr^{-1}$)	0.107	0.429	0.067	0.653
Modern lake sediment Hg_T ($g \cdot yr^{-1}$)	0.61	1.26	0.20	0.17
Direct wet Hg_T deposition / lake sediments	2%	8%	31%	6%
Potential-indirect wet Hg_T deposition (runoff) / lake sediments	18%	34%	34%	38%
Unaccounted-for Hg_T source to lake sediments	80%	58%	35%	56%

Table 5. Spatial correlation among studied lakes to further infer modern atmospheric Hg deposition source apportioning across California. R represents simple-correlation coefficient.

Lake Comparison	**Castle Lake** Regional Hg Belt Source	**Island Lake** Regional Mine Source	**Emerald Lake** Regional Background
Wildcat Lake	R = 0.79	R = 0.73	R = 0.42
Castle Lake		R = 0.83	R = 0.84
Island Lake			R = 0.37

Table 6. Summary of atmospheric wet Hg deposition studies in California.

Site	n	Volume-Weighted Hg (ng/L)	Annual Rainfall (cm)	Flux (ug·m^{-2}·yr^{-1})	Reference
MDN Site CA72 (Moffett Field, CA)	124	9			MDN (CA72)
MDN Site CA75 (Sequoia National Park)	57	6			MDN (CA75)
MDN Site CA97 (Covelo)	58	4			MDN (CA97)
SF Bay Estuary	59	8	53	4.2	Tsai and Hoenicke (2001)
Long Marine Laboratory (LML)	17	6	~67a	4	Steding and Flegal (2002)
Moffett Field (MF)	26	11.8	~37 a	4.4	Steding and Flegal (2002)
Pt. Reyes National Seashore	15	5.5b	51	2.8	Choe et al. (2006)
Twitchell Island, SF Bay-Delta	13	4.4b	41	1.8	Choe et al. (2006)
Woodland, Central Valley	19	4.3b	54	2.3	Choe et al. (2006)

Table 7. California particulate Hg_T concentrations comparing proposed mining and atmospheric sources to Central California water bodies. Foe-Calfed data from Churchill and Clinkenbeard, 2003.

Location	Source	Matrix	Proposed Hg Source	Annual Average Hg_T (ng.g^{-1})
Mokelumne-Consumnes Rivers	Foe, Calfed	Particulates	Mine tailings	335
Prospect Slough	Foe, Calfed	Particulates	Mine tailings	229
Putah Creek	Foe, Calfed	Particulates	Mine tailings	350
State Water Project.	Foe, Calfed	Particulates	Mine tailings	198
Greene's Landing, SR	Foe, Calfed	Particulates	Mine tailings	171
Vernalis, SJ	Foe, Calfed	Particulates	Atmospheric	124
Delta Mendota Canal	Foe, Calfed	Particulates	Atmospheric	141
Staten Island	Foe, Calfed	Particulates	Atmospheric	120
Empire Tract	Foe, Calfed	Particulates	Atmospheric	77
Twitchell Island Drain	Foe, Calfed	Particulates	Atmospheric	54
Upper Jones Main Drain	Foe, Calfed	Particulates	Atmospheric	60
Wildcat Lake	This Study	Surficial Sediment	Atmospheric	89
Castle Lake	This Study	Surficial Sediment	Atmospheric	141
Island Lake	This Study	Surficial Sediment	Atmospheric	121
Emerald Lake	This Study	Surficial Sediment	Atmospheric	115
Clear Lake	Suchanek *et al.* 1997	Surficial Sediment	Mine tailings	400
Lake Tahoe	Heyvaert *et al.* 2000	Surficial Sediment	Atmospheric	200
San Fransisco Bay	Hornberger *et al.* 1999	Surficial Sediment	Mine tailings	300

Figure 1. Location of study lakes, gold mines and Hg mines in California. Shapefiles courtesy of USGS mine reclamation and the Land Conservation Department of California.

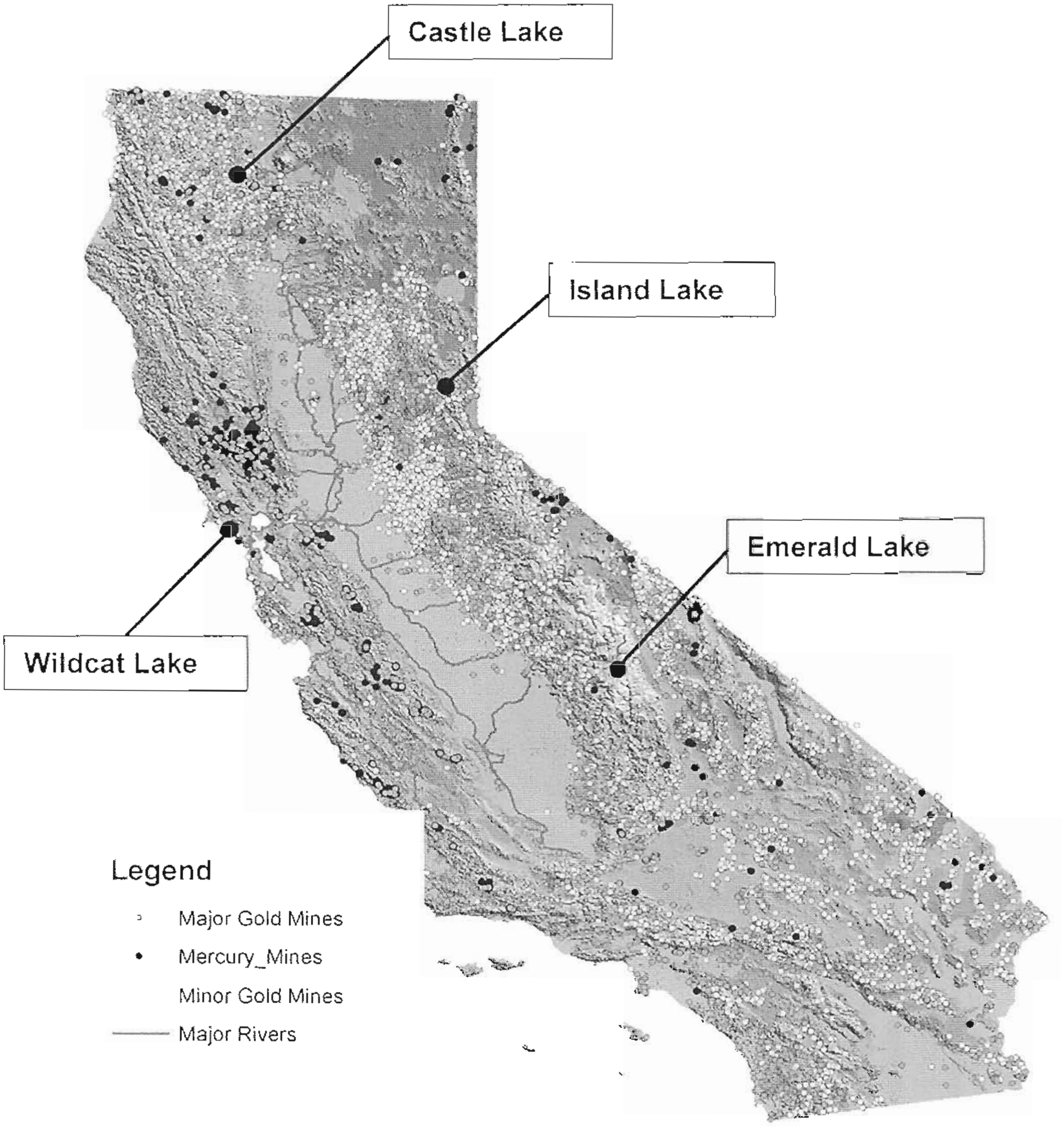
Castle Lake
Island Lake
Emerald Lake
Wildcat Lake
Legend
Major Gold Mines
Mercury_Mines
Minor Gold Mines
Major Rivers

Figure 2. Wildcat Lake aerial map, bathymetry map indicating sampling locations, and photograph of lake.

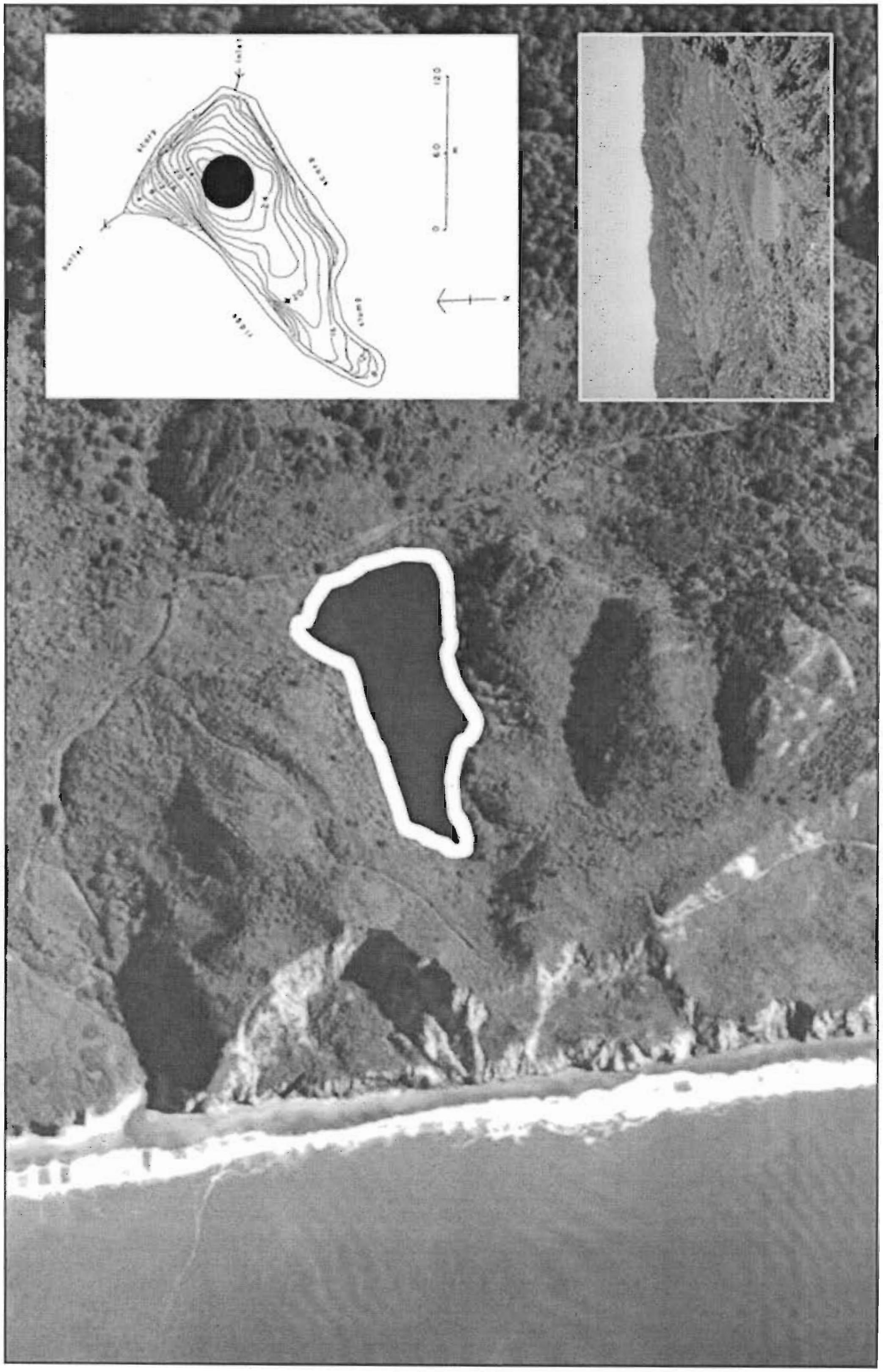
inlet
steep
grass
24
20
outlet
ridge
stumps
0
60
120
m
N

Figure 3. Castle Lake aerial map, bathymetry map indicating sampling locations, and photograph of lake.

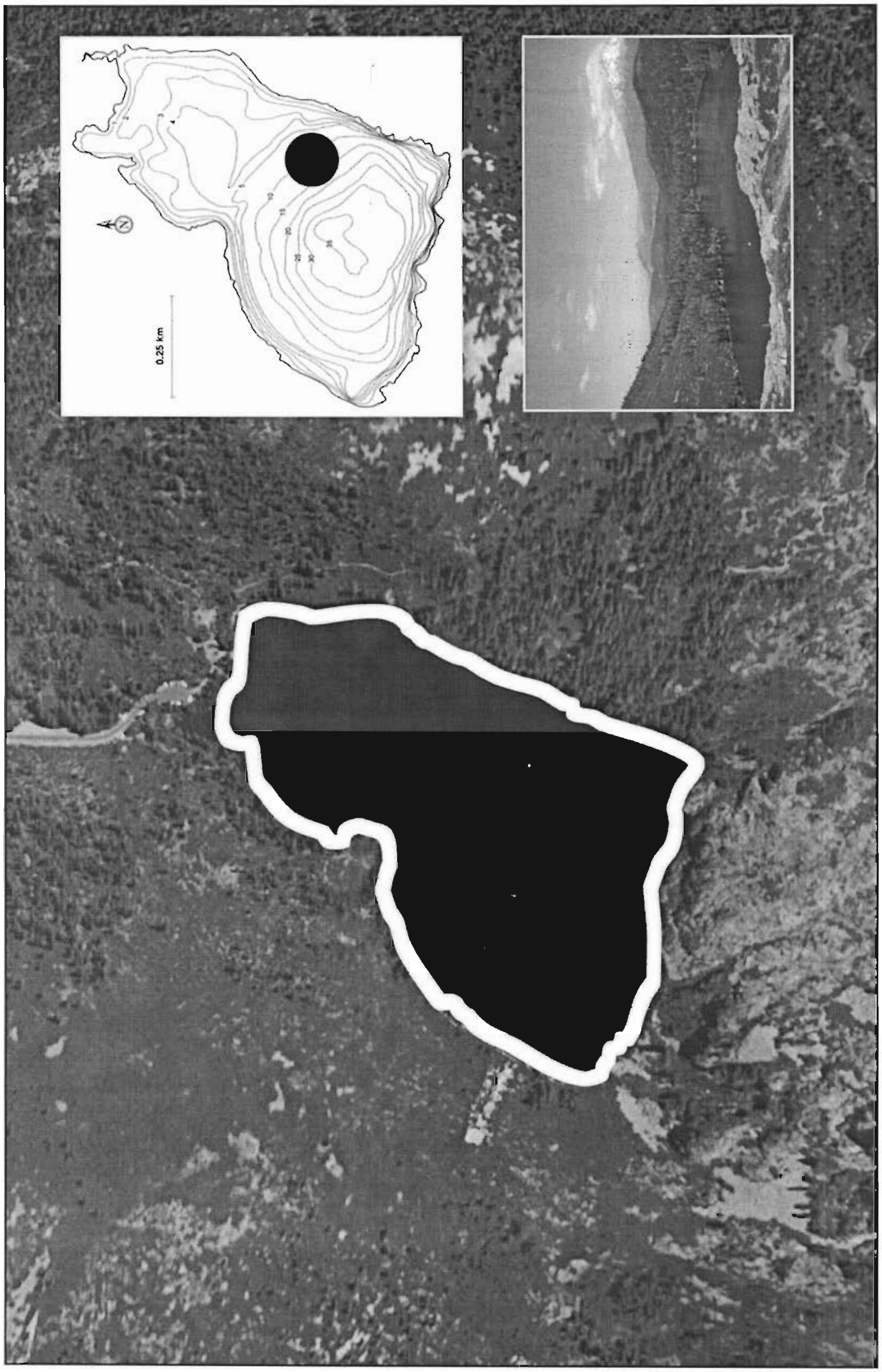
N
0.25 km

Figure 4. Island Lake aerial map, bathymetry map indicating sampling locations, and photograph of lake.

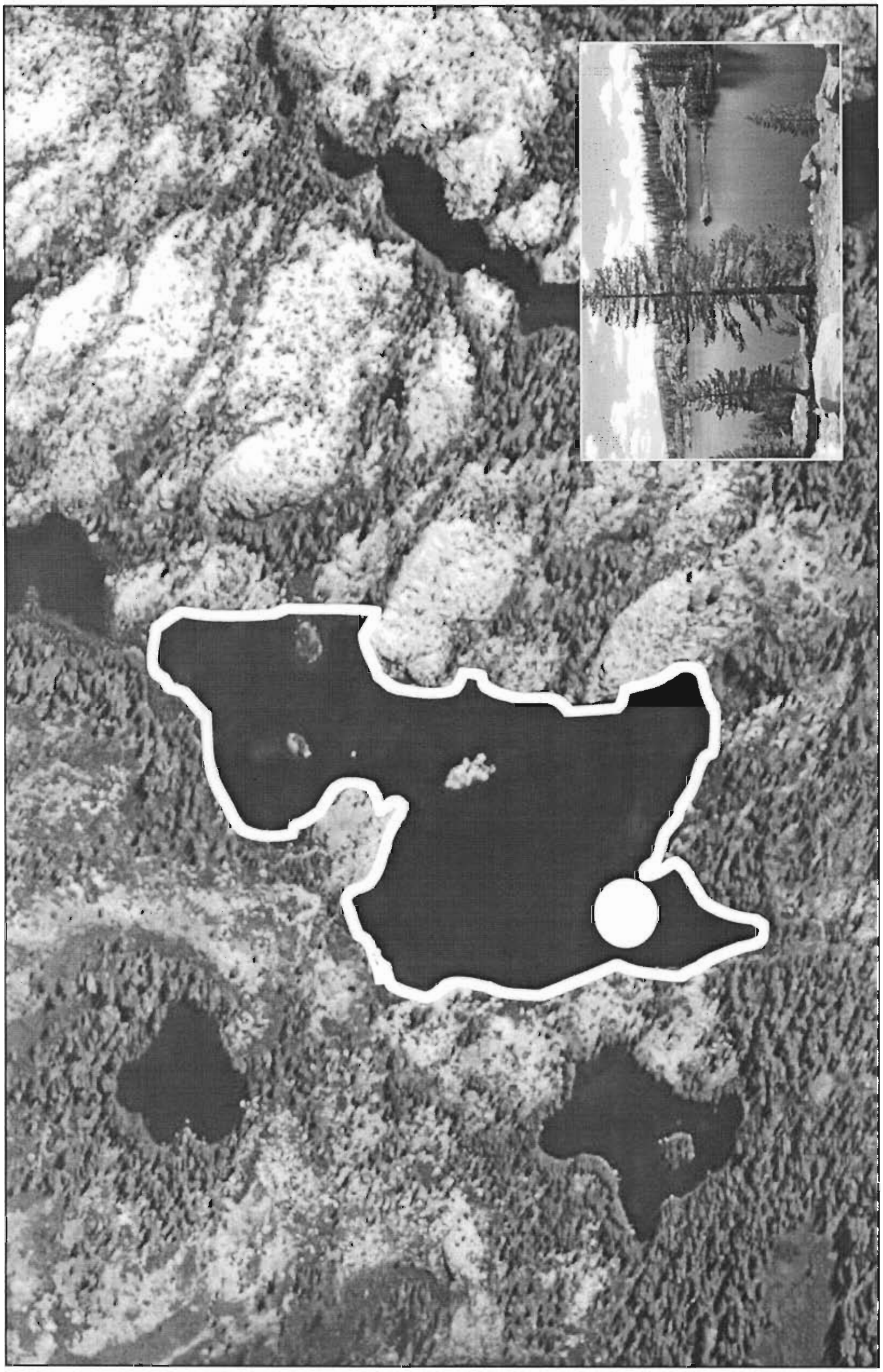

Figure 5. Emerald Lake aerial map, bathymetry map indicating sampling locations, and photograph of lake.

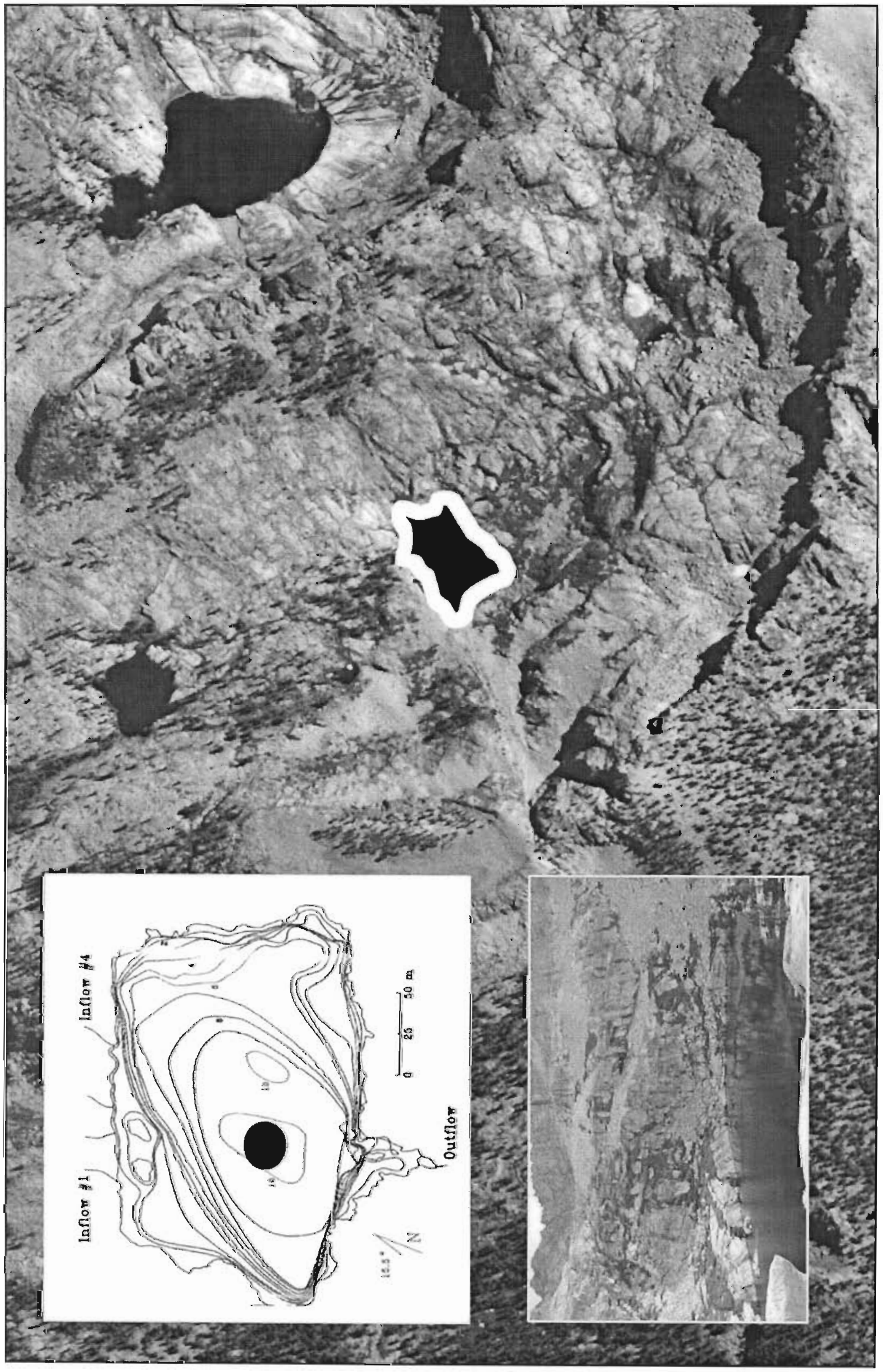
Inflow #1
Inflow #4
Outflow
0 25 50 m
10.5°
N

Figure 6. A schematic demonstrating how to apply a tailing correction to the ^{208}Po and ^{209}Po spike and native ^{210}Po activity peaks.

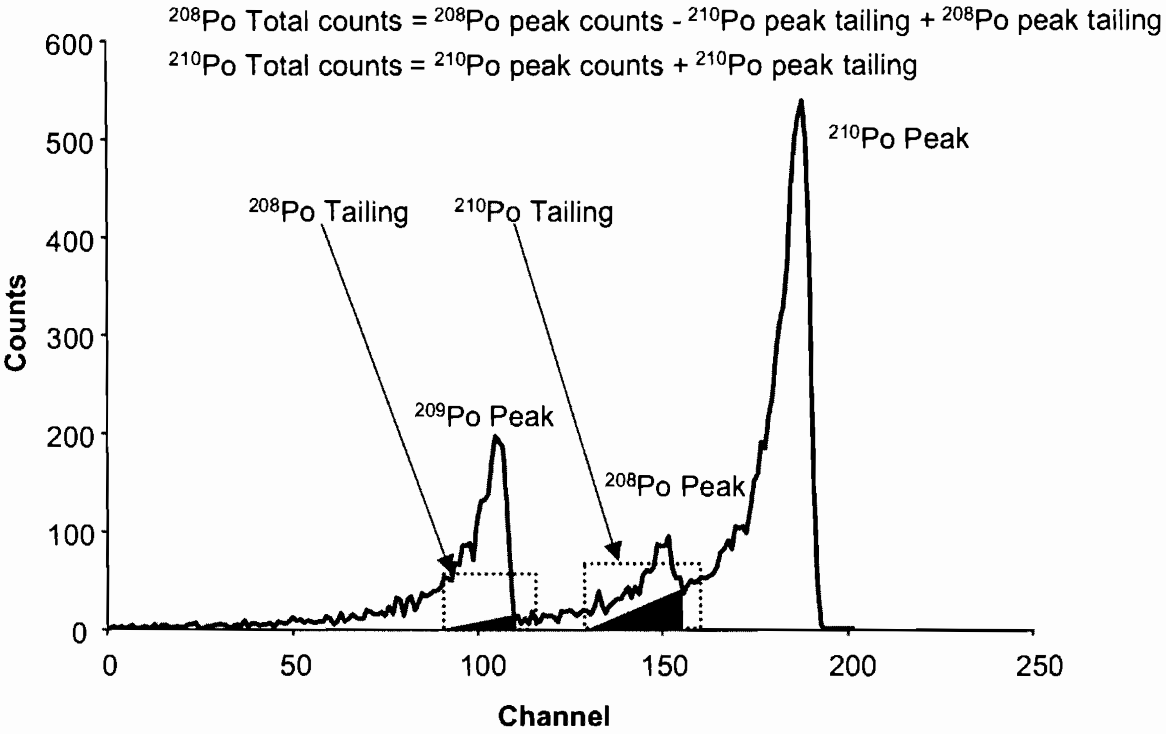
^{208}Po Total counts = ^{208}Po peak counts - ^{210}Po peak tailing + ^{208}Po peak tailing
^{210}Po Total counts = ^{210}Po peak counts + ^{210}Po peak tailing
^{210}Po Peak
^{208}Po Tailing
^{210}Po Tailing
^{209}Po Peak
^{208}Po Peak
Counts
600
500
400
300
200
100
0
0
50
100
150
200
250
Channel

Figure 7. A schematic demonstrating the method for determining the error associated when using the natural log of the $^{210}Pb_{ex}$ slope (m) to calculate sedimentation rate (s) with highly variable surficial lake ^{210}Pb activities.

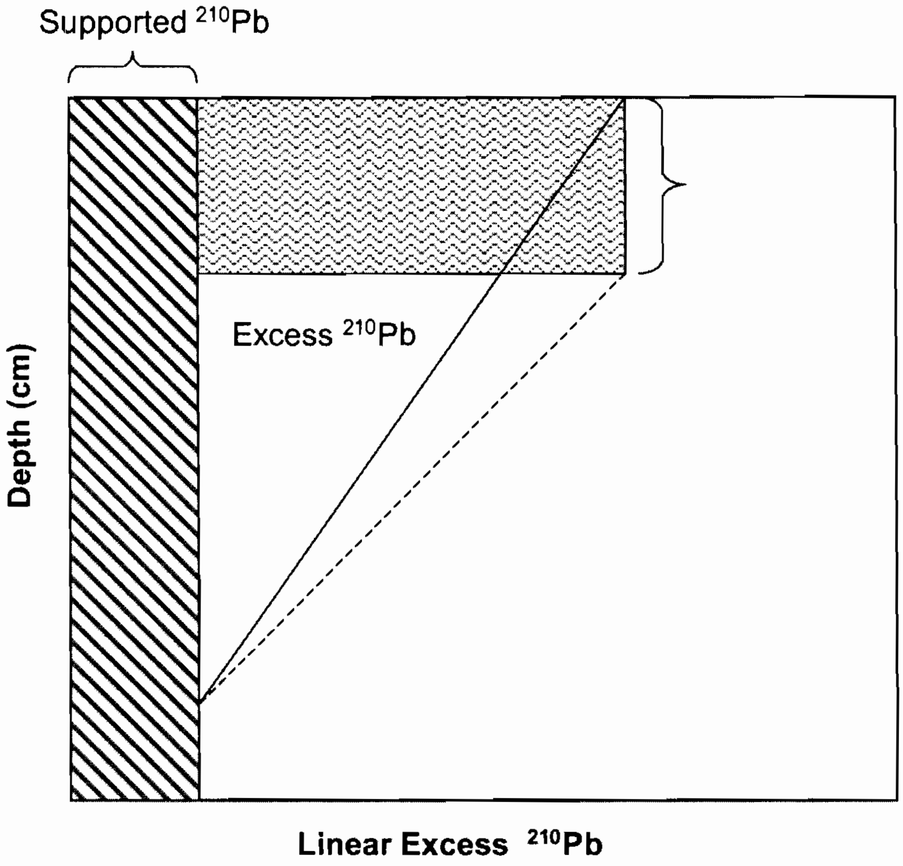
Supported ^{210}Pb
Excess ^{210}Pb
Depth (cm)
Linear Excess ^{210}Pb

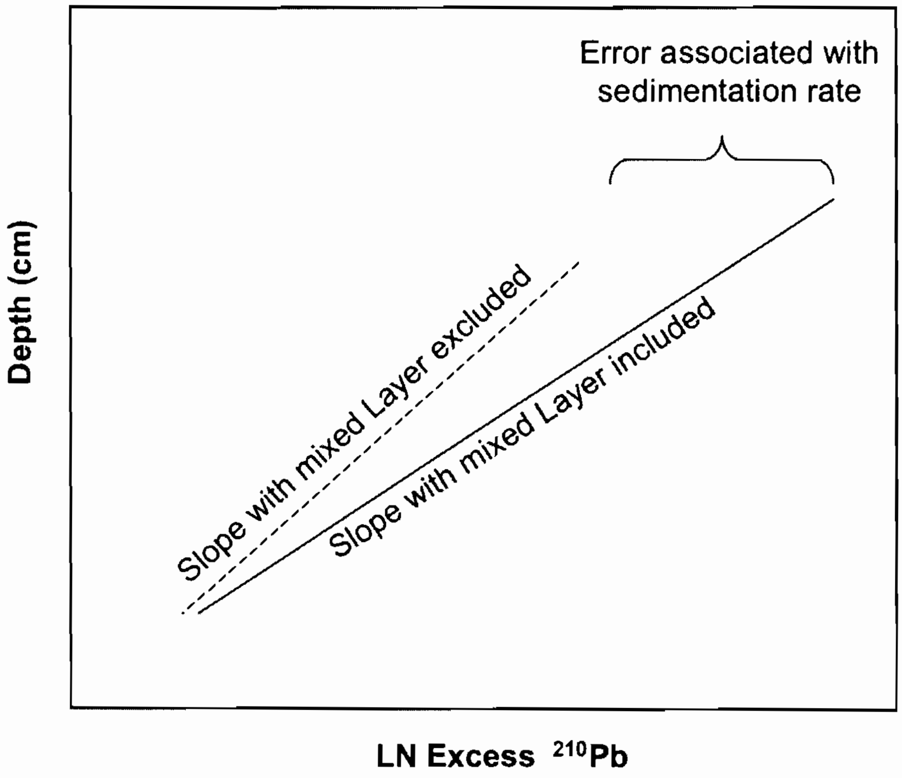
Error associated with sedimentation rate
Slope with mixed Layer excluded
Slope with mixed Layer included
Depth (cm)
LN Excess ^{210}Pb

Figure 8. Wildcat Core 1(a), Core 2 (b), and Core 3 (c) Linear and LN $^{210}Pb_{ex}$ lake sediment profiles. Error bars on linear $^{210}Pb_{ex}$ profiles represent the cumulative analytical error (σ) the dashed error lines on the LN $^{210}Pb_{ex}$ profiles represent 95% confidence intervals of the regression.

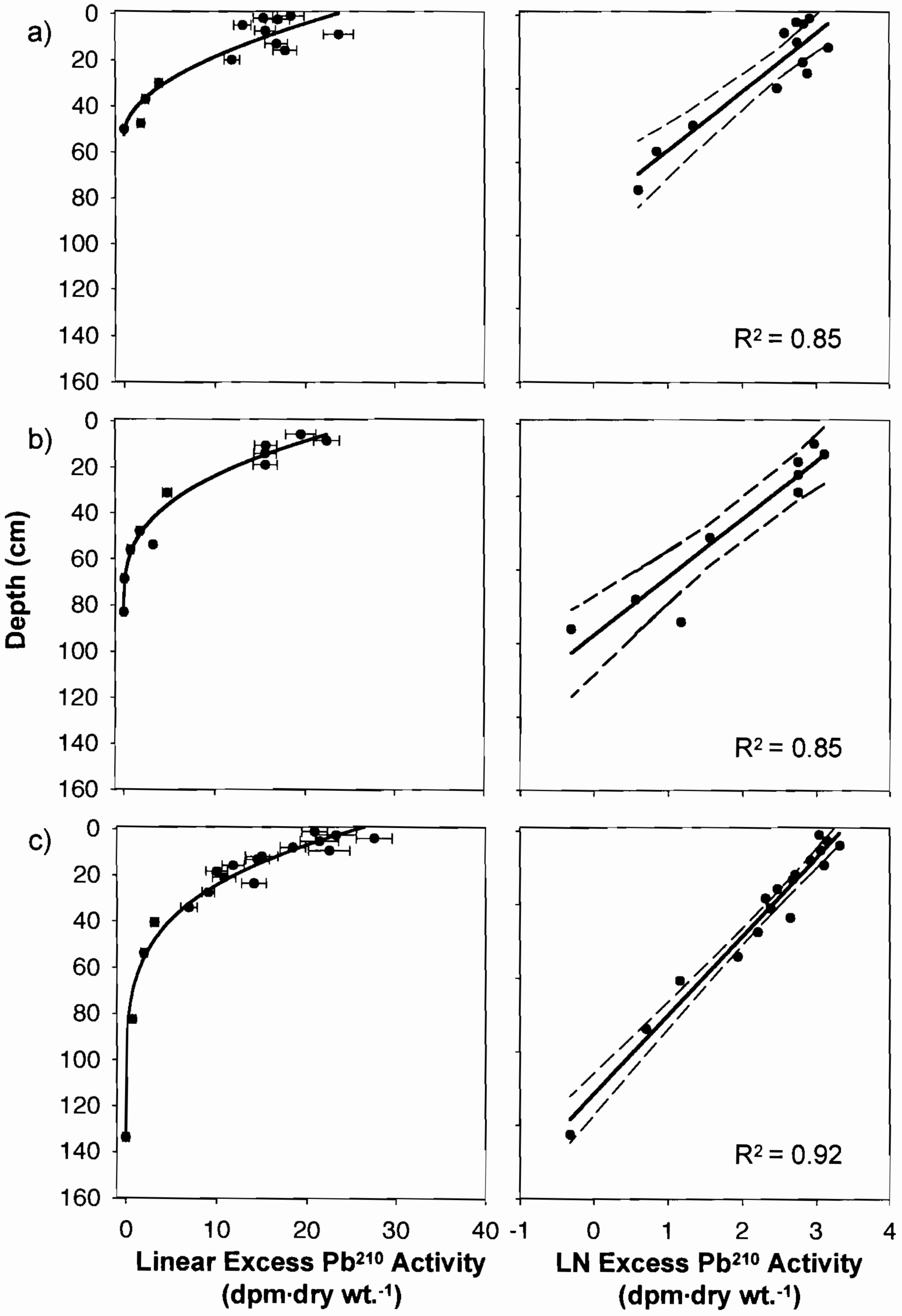
a)
b)
c)
Depth (cm)
0
20
40
60
80
100
120
140
160
R² = 0.85
R² = 0.85
R² = 0.92
0
10
20
30
40
-1
0
1
2
3
4
Linear Excess Pb210 Activity (dpm·dry wt.-1)
LN Excess Pb210 Activity (dpm·dry wt.-1)

Figure 9. Castle Core 1 (a), Island Core 1 (b), and Emerald Core 1 (c) Linear and LN $^{210}Pb_{ex}$ lake sediment profiles. Error bars on linear $^{210}Pb_{ex}$ profiles represent the cumulative analytical error (σ) and the dashed error lines on the LN $^{210}Pb_{ex}$ profiles represent 95% confidence intervals of the regression.

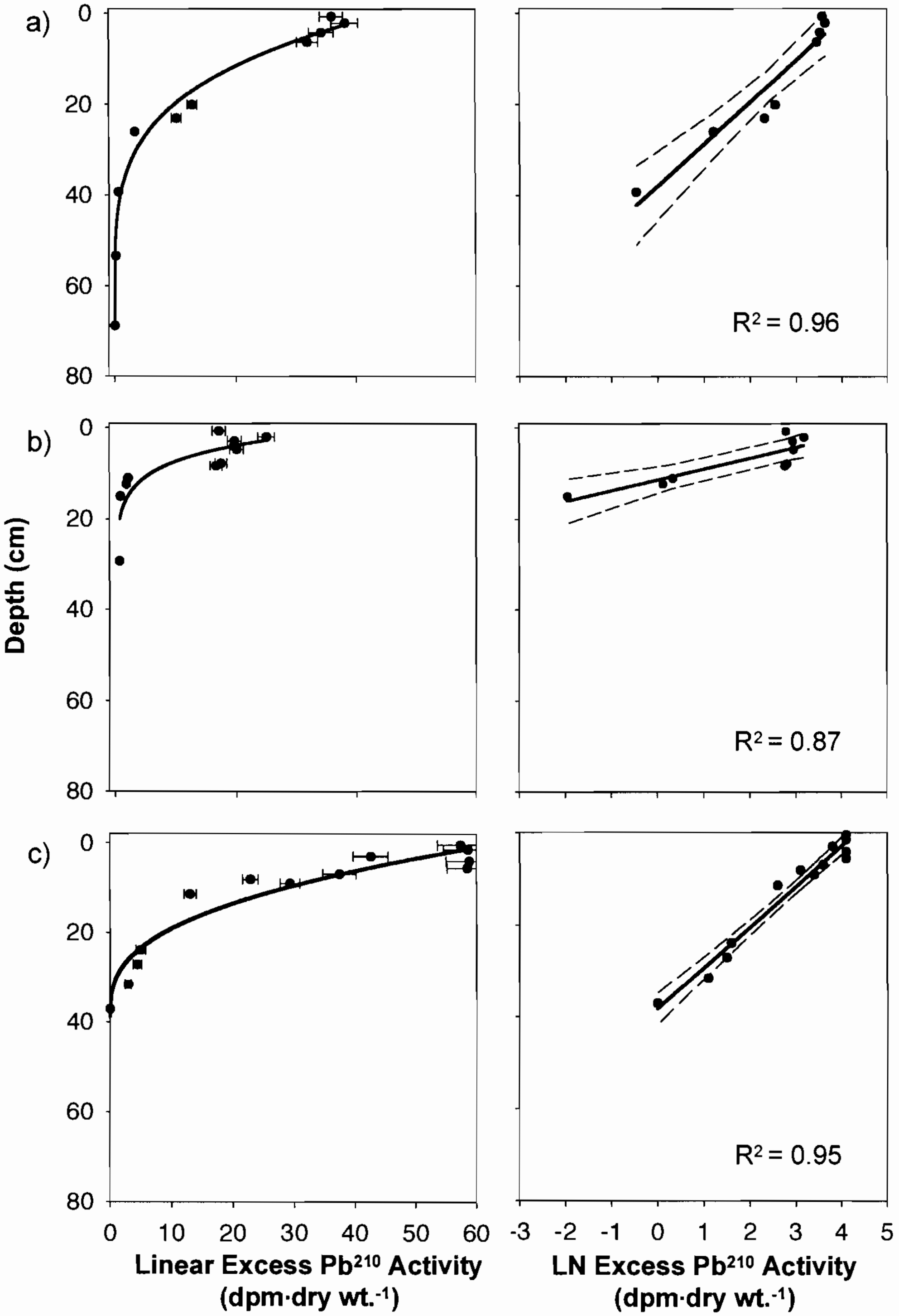a)
b)
c)
Depth (cm)
0
20
40
60
80
R² = 0.96
R² = 0.87
R² = 0.95
0
10
20
30
40
50
60
-3
-2
-1
0
1
2
3
4
5
Linear Excess Pb²¹⁰ Activity (dpm·dry wt.⁻¹)
LN Excess Pb²¹⁰ Activity (dpm·dry wt.⁻¹)

Figure 10. Wildcat (a), Castle (b), Island (c), and Emerald (d) Hg_T lake sediment profiles indicating modern and ^{210}Pb determined pre-anthropogenic or historic (<1850 yr.) Hg_T concentrations.

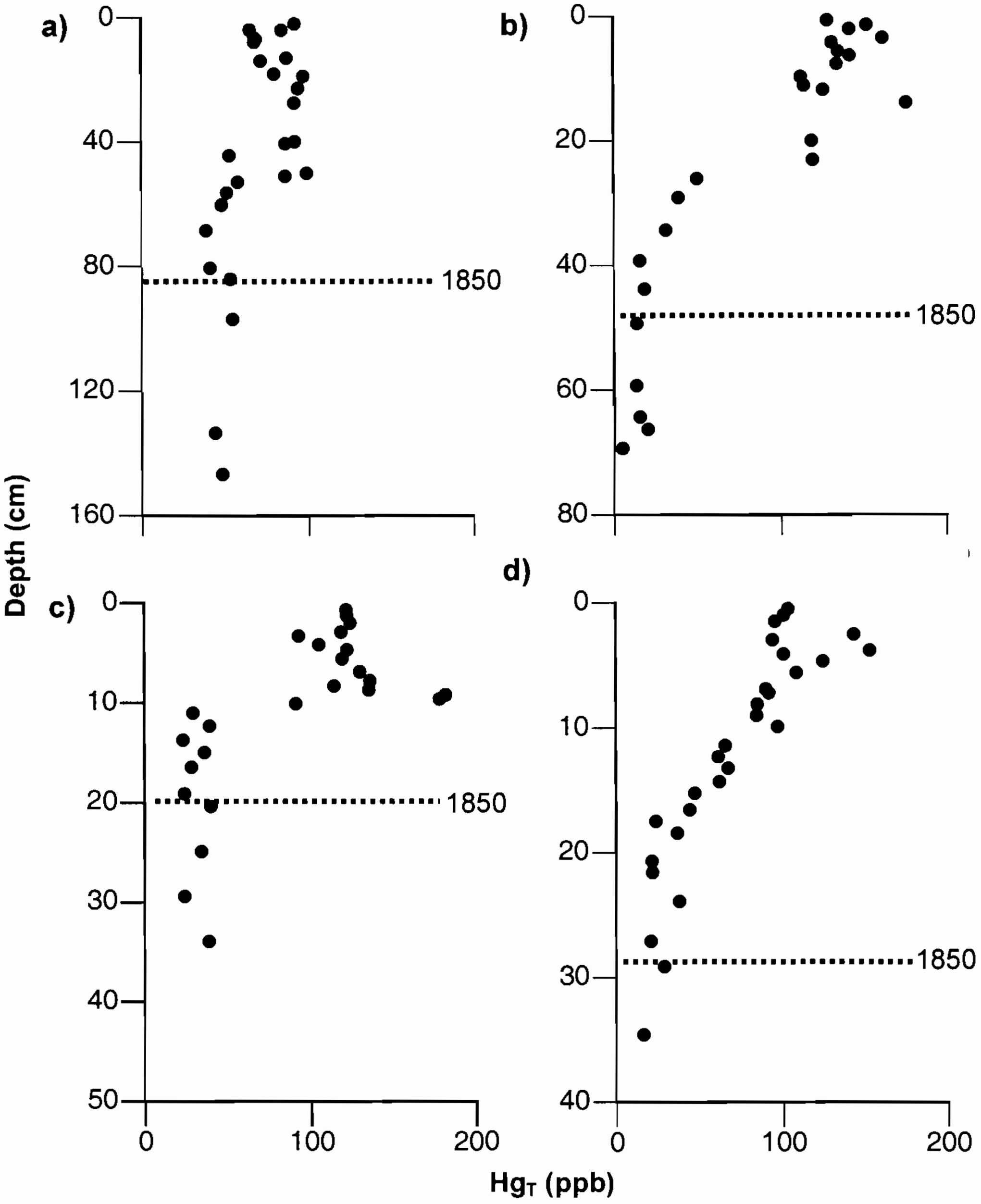
a)
b)
c)
d)
Depth (cm)
Hg_T (ppb)
0
40
80
120
160
0
20
40
60
80
0
10
20
30
40
50
0
10
20
30
40
0
100
200
0
100
200
1850
1850
1850
1850

Figure 11. Particle size interpolation verification using photomicroscopy qualitative analysis. An example of two sediment samples from Castle Lake (core 2) composed of diatoms and amorphous organic material at 1 cm dry depth and episodic increases in grain size and mineral composition at 14 cm dry depth. The photomicroscopy is used to define the particle size analysis interpolation of diatoms (<50 μm) and larger grains and minerals (51-200 μm). The shaded areas demonstrate volume changes between the diatom and mineral size ranges.

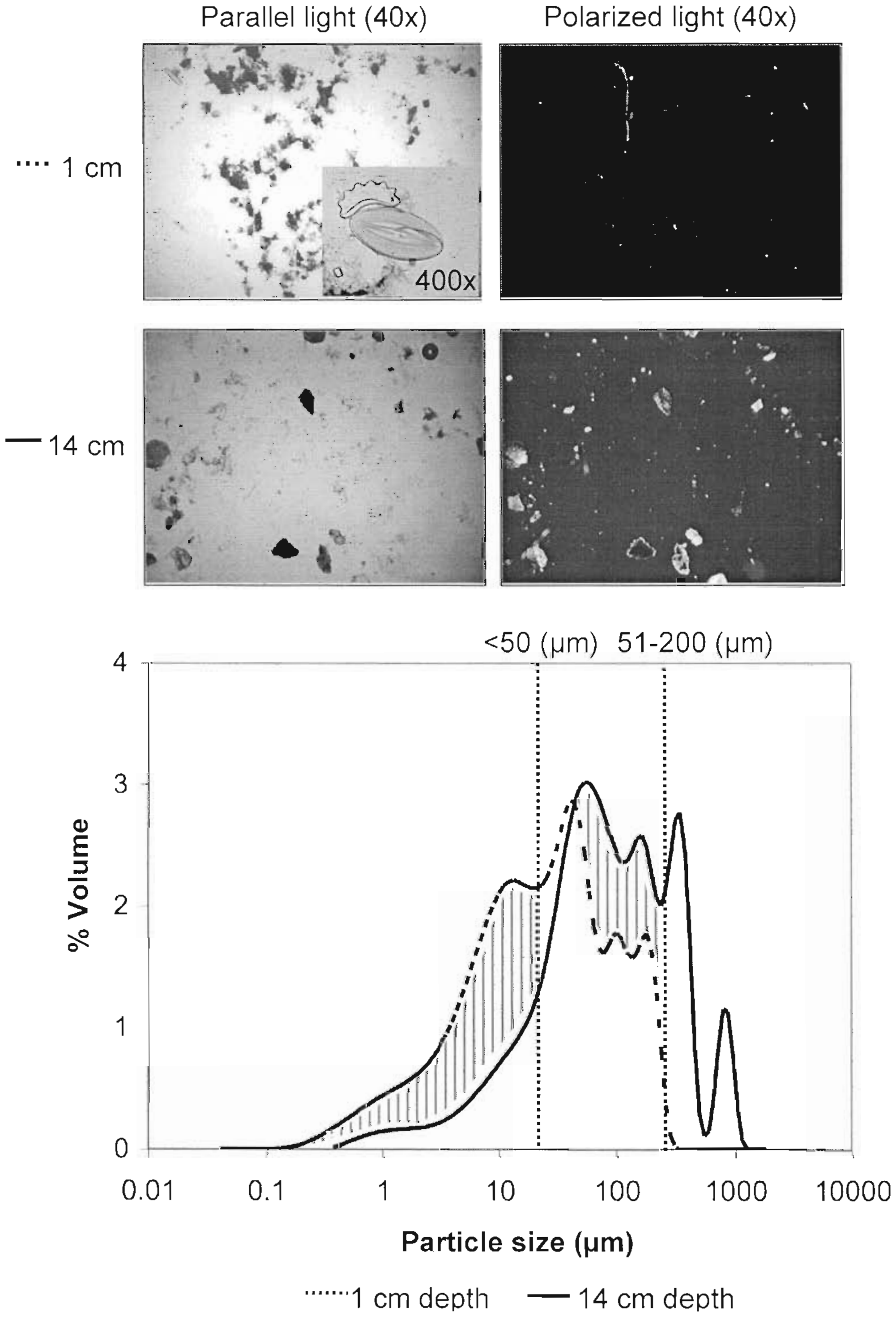
Parallel light (40x)
Polarized light (40x)
1 cm
400x
14 cm
<50 (μm)
51-200 (μm)
4
3
2
1
0
% Volume
0.01
0.1
1
10
100
1000
10000
Particle size (μm)
1 cm depth
14 cm depth

Figure 12. Wildcat (a), Castle (b), Island (c), and Emerald (d) sediment profiles presenting interpolated % volume of <50 and 51-200 μm particle diameter.

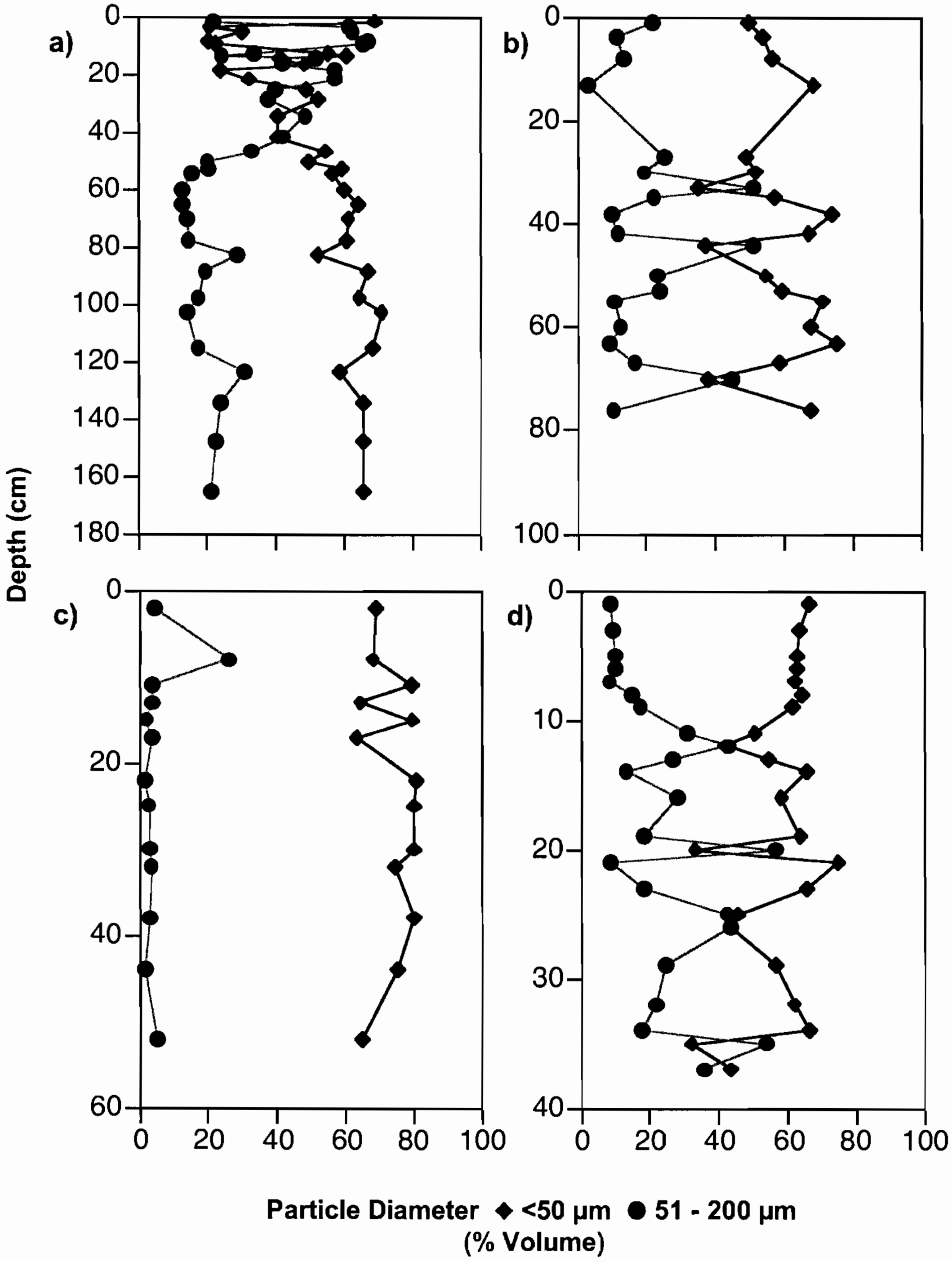
a)
b)
c)
d)
Depth (cm)
0
20
40
60
80
100
120
140
160
180
0
20
40
60
80
100
0
20
40
60
0
10
20
30
40
0
20
40
60
80
100
0
20
40
60
80
100
Particle Diameter ◆ <50 µm ● 51 - 200 µm
(% Volume)

Figure 13. Wildcat (a), Castle (b), Island (c), and Emerald (d) magnetic susceptibility lake sediment profiles.

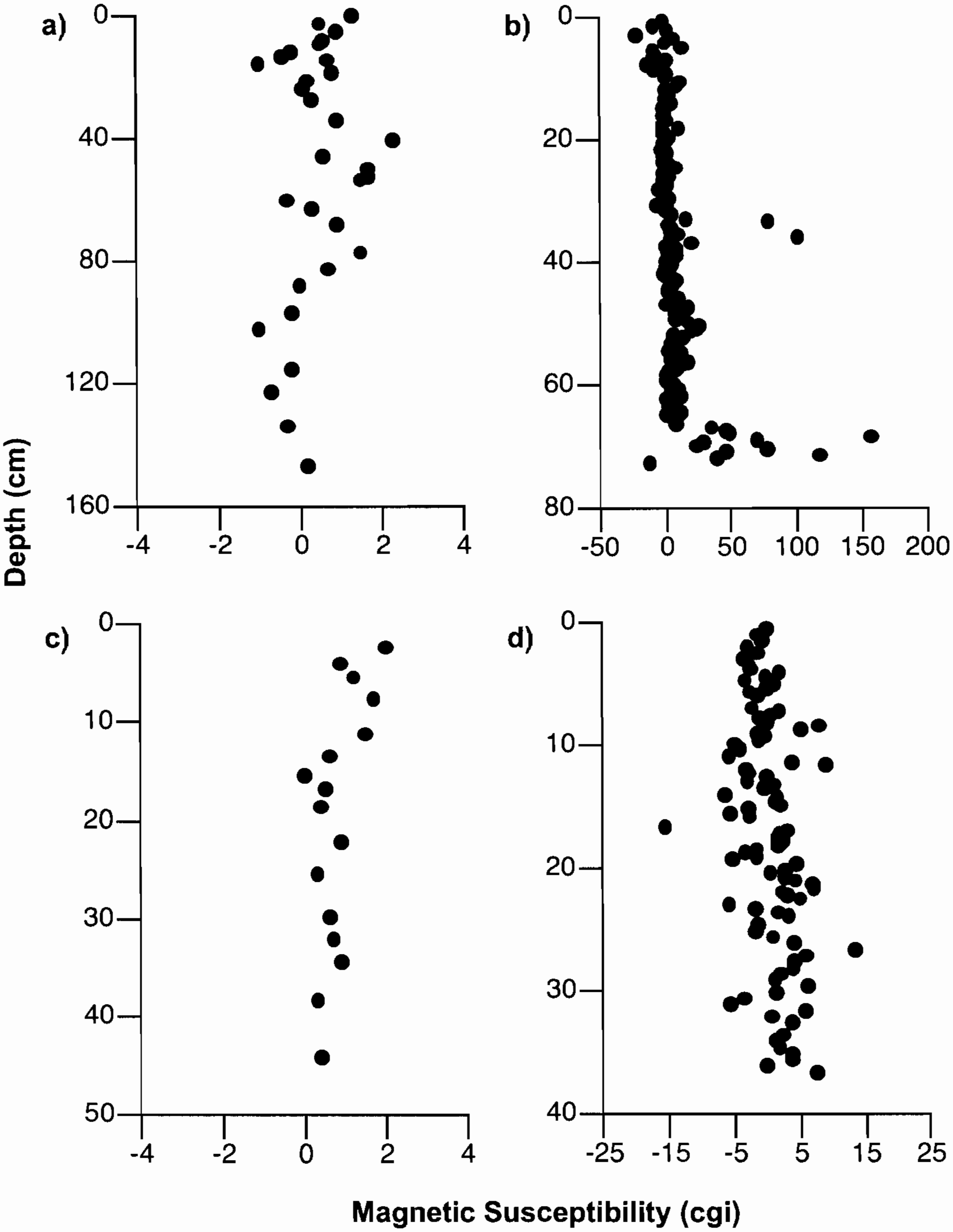a)
b)
c)
d)
0
40
80
120
160
-4
-2
0
2
4
0
20
40
60
80
-50
0
50
100
150
200
0
10
20
30
40
50
-4
-2
0
2
4
0
10
20
30
40
-25
-15
-5
5
15
25
Depth (cm)
Magnetic Susceptibility (cgi)

Figure 14. Wildcat (a), Castle (b), Island (c), and Emerald (d) particulate organic carbon and nitrogen profiles. The Carbon/Nitrogen is presented as a ratio and the POC and PON are % weights.

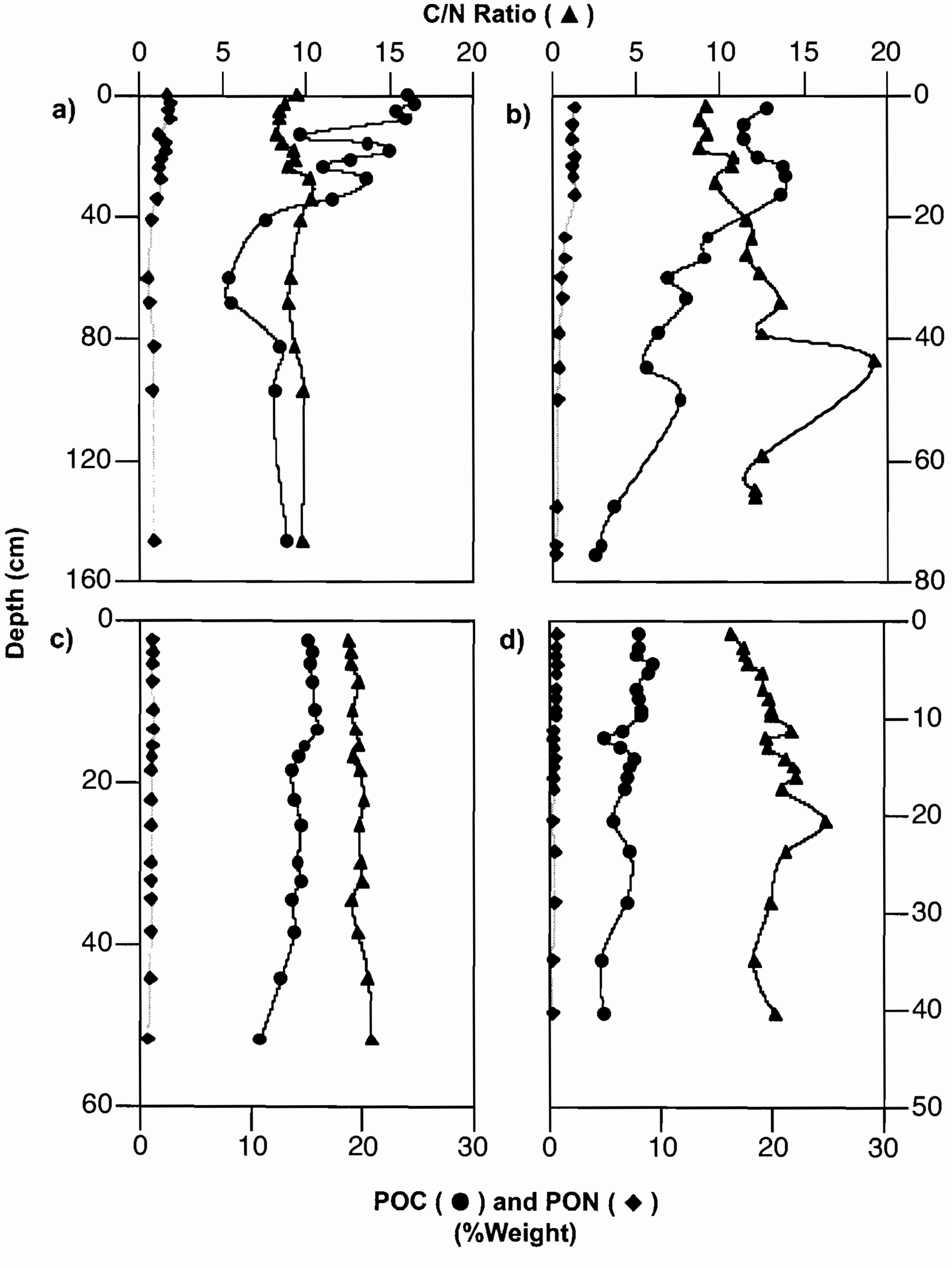
C/N Ratio (▲)
0
5
10
15
20
0
5
10
15
20
a)
b)
c)
d)
0
40
80
120
160
0
20
40
60
80
0
20
40
60
0
10
20
30
40
50
Depth (cm)
0
10
20
30
0
10
20
30
POC (●) and PON (◆)
(%Weight)

Figure 15. Standardized Hg and watershed component regression analysis.

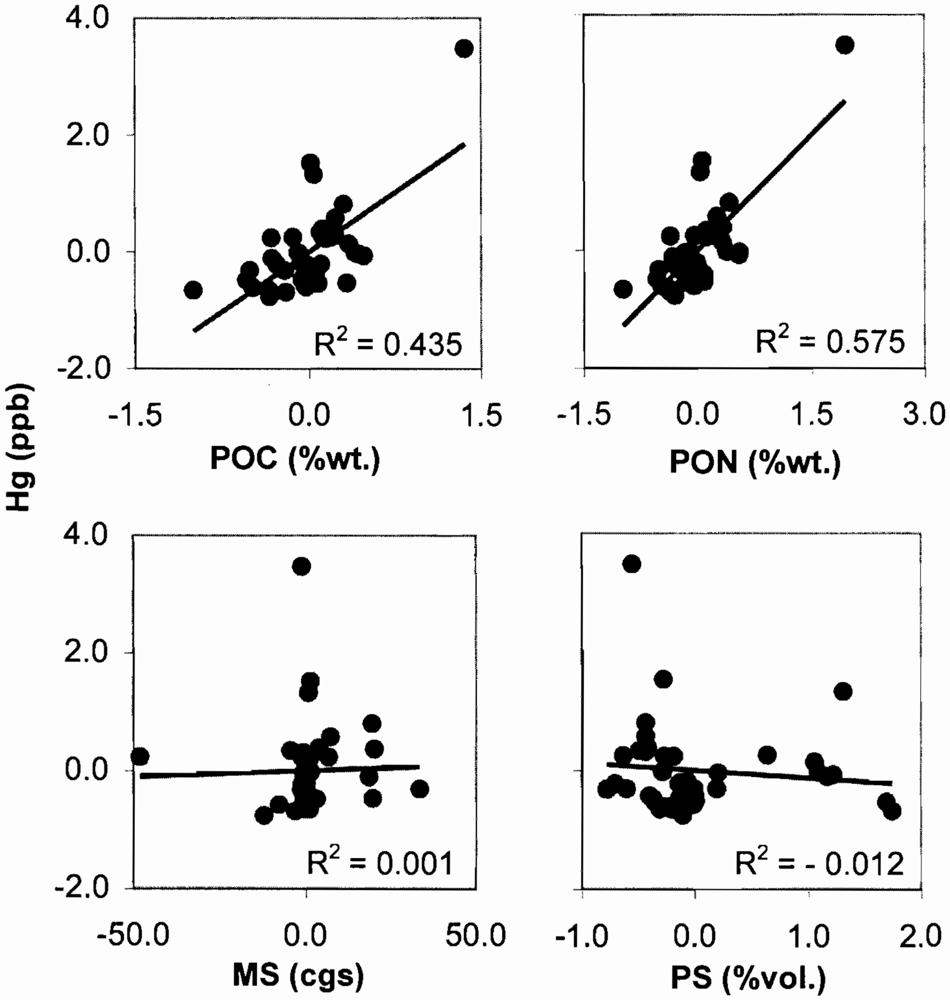
Hg (ppb)
4.0
2.0
0.0
-2.0
R^2 = 0.435
-1.5
0.0
1.5
POC (%wt.)
R^2 = 0.575
-1.5
0.0
1.5
3.0
PON (%wt.)
4.0
2.0
0.0
-2.0
R^2 = 0.001
-50.0
0.0
50.0
MS (cgs)
R^2 = - 0.012
-1.0
0.0
1.0
2.0
PS (%vol.)